Structural Characteristics of Biodegradable Thermoplastic Starch/Poly(ethylene–vinyl alcohol) Blends

STEPHANIE SIMMONS and EDWIN L. THOMAS*

Program in Polymer Science and Technology, Department of Chemical Engineering, Department of Materials Science and Engineering, Massachusetts Institute of Technology, Cambridge, Massachusetts 02139

SYNOPSIS

To establish relationships among the blend composition, processing history, and the resultant properties of starch-based thermoplastics, three varieties of corn starch: (1) Waxy Maize, (2) Native Corn, and (3) high-amylose Hylon VII were extrusion-blended with poly(ethylene–vinyl alcohol) (EVOH) containing 56 mol % VOH. Wide-angle X-ray scattering (WAXS), differential scanning calorimetry (DSC), scanning electron microscopy (SEM), and transmission electron microscopy (TEM) were used to examine the structural characteristics of the blends. All starches were destructurized upon compounding and a fine dispersion was achieved with EVOH. The Native Corn and Hylon VII blends were phase-separated and exhibited some miscibility between the polymer components as evident in EVOH melting-point depression, smaller domain sizes, lower contrast between phases in TEM, and increased resistance to moisture and enzyme-etching treatments. Starches containing amylose exhibited complexation and crystallinity in the starch fraction, although most of the crystallinity in the blends was due to the EVOH component. Waxy Maize blends were well phase-separated with larger domain sizes and underwent phase coarsening as a function of time in the melt. When subjecting the blends to capillary flow, orientation of both starch-rich and EVOH-rich domains was observed at various compositions, with the EVOH component undergoing significantly more orientation relative to starch as evident by the presence of EVOH-rich fibrils. Finally, EVOH was found to coat the surfaces of filaments produced from the blends even at rather high levels of starch (70%), which is expected to improve moisture sensitivity and slow down the initial rate of biodegradation.

INTRODUCTION

Starch has been considered as a candidate material in certain thermoplastic applications because of its known biodegradability, availability, and low cost.[1,2] Its utilization in nonfood, plastic applications has been investigated by researchers over the past 50 years.[3–20] Reviews of these developments have been published by Roper and Koch,[21] Doane,[22] Shogren et al.,[23] and others.[24–26] Over the last few years, corporations such as Novamont Inc., a subsidiary of the Montedison Group in Italy, and the Warner-Lambert Co., Morris Plains, NJ, have commercially produced various grades of starch-based thermoplastic resin (marketed under the names, Mater-Bi® and Novon®, respectively). In the production of these materials, heat, moisture, and mechanical deformation are used to destructurize starch and blend it with various polymers and plasticizers in order to achieve a fine dispersion.[4,15,27–29] Typical applications of these blends are food utensils, disposable pens, packaging for peanuts, composting bags, and other single-use items. The key to understanding how to optimize these product properties is establishing the relationships among the blend composition, processing history, and the resultant structural and physical properties of such materials.

Starch itself is not a true thermoplastic in the sense that it will degrade when heated and not form a melt on its own. Combining starch with plasticizers such as glycerin and water, however, will make starch behave as a thermoplastic. In this state, it

* To whom correspondence should be addressed.

Journal of Applied Polymer Science, Vol. 58, 2259–2285 (1995)
 CCC 0021-8995/95/122259-27

can flow as a melt through an extruder and be processed in typical thermoplastic applications. Unfortunately, the mechanical properties and dimensional stability of articles made solely of thermoplastic starch are very dependent upon the relative humidity at which these articles are stored.[30] One way of overcoming this problem is to blend starch with other polymers that possess more stable properties and some degree of biodegradability. In the present study, poly(ethylene-*co*-vinyl alcohol) (EVOH) containing 56 mol % vinyl content was used. The addition of this synthetic component serves to improve the processability, increase the toughness, and ameliorate the moisture instability of the product, but will also decrease the overall rate of biodegradability of the system (EVOH biodegrades, although on a time scale much slower than that of starch[26,31]). Previous studies focusing on the injection-molding and fiber-spinning capabilities, physical properties, and rheology of these particular blends have been performed.[30,32,33] An in-depth transmission electron microscopy (TEM) study of the morphology of starch-based blends has also recently been performed.[34]

Since there are many sources of starch and each of these exhibits different characteristics, three different varieties of corn starch were chosen for study. These starches, which include a Native Corn starch and two hybrid corn starches (Waxy Maize and Hylon VII), differ in the percentage of linear amylose to branched amylopectin that exist in each starch granule and in the corresponding molecular weights of these polymer components. The blend morphology that results upon processing these starch varieties with EVOH will not only influence the mechanical properties but also the manner in which a product made from these materials degrades. For example, crystallinity will decrease the accessibility of moisture and, hence, microbes to certain areas within the blend. Also, whether or not the starch forms a continuous phase or discrete domains within the EVOH component and the size of these domains will effect both the biodegradation rate and the mechanical behavior. Finally, the biodegradation rate will be strongly affected if there is surface enrichment by one component.

The processability and properties of any thermoplastic blend will depend strongly upon the morphology that results from both the thermodynamics and kinetics involved in the mixing process.[35] The blending of different starch varieties with EVOH requires the destruction of highly organized granules of the Native Corn and Waxy Maize starches or deorganization of the relatively amorphous, pretreated high-amylose particles (Hylon VII). These raw materials range in size from 5 to 25 μm. EVOH pellets of about 3 mm in diameter and 4 mm in length must be melted and thoroughly blended with the starch domains. Whether or not softening of the EVOH phase occurs prior to, during, or after the granule destructurization and/or softening of the starch will influence the morphology of the blend upon exiting the extruder. Water (both in the "dry" materials and as a liquid feed) will cause the starch granules to swell; further destructurization occurs with the application of heat and shear. In addition, water as well as glycerin, injected into the extruder as a relatively nonvolatile plasticizer, may partition unevenly between the starch and EVOH components. Processing additives, such as triglycerides, may also effect processing by lowering the interfacial tension between phases in the melt and, hence, the final blend morphology. The number of variables involved during the compounding of starch/EVOH blends makes this a very complex process which is expected to lead to varied morphologies and associated properties.

The present study is a structural investigation of a systematic series of model blends consisting of starch, a synthetic polymer, and plasticizers, conducted using wide-angle X-ray scattering (WAXS), differential scanning calorimetry (DSC), and scanning electron microscopy (SEM). Selected results from a transmission electron microscopy (TEM) study are also presented, but they are discussed in detail in a separate article.[34] X-ray scattering was used to determine crystalline phase types, physical aging effects in the blends, and crystallinity changes with temperature and time. DSC was employed to explore thermal behavior (e.g., T_m and T_g of various components) and perhaps gain information on the miscibility of the blend. Electron microscopy was used to examine the morphology of the blends as a function of starch type and EVOH composition. The effect of capillary flow on certain blends was investigated using SEM to gain insight in the flow properties of the starch and EVOH components. Finally, a melt phase size coarsening study was also performed to examine the stability of the melt for starch/EVOH blends. A discussion of the significance of these structural observations on the processability, biodegradability, and mechanical properties of starch-based thermoplastics is presented.

EXPERIMENTAL

Raw Materials

Amioca, Melojel, and EK Fl. Hylon VII starches were supplied by National Starch and Chemical Co.

(Bridgewater, NJ). Amioca Waxy Maize (WM) is a hybrid corn starch containing essentially 100% highly branched amylopectin ($M_{AP} \sim 100 \times 10^6$ g/mol). Melojel is a Native Corn starch (NC) possessing 28% of linear amylose ($M_{AM} \sim 1 \times 10^6$ g/mol) and 72% amylopectin ($M_{AP} \sim 50$–100×10^6 g/mol). Both the WA and NC starches were received in the form of granules before compounding. Hylon VII (HY) is a genetically engineered corn starch which consists of approximately 70% amylose ($M_{AM} \sim 0.8 \times 10^6$ g/mol) and 30% amylopectin ($M_{AP} \sim 20$–50×10^6 g/mol). The HY starch, as supplied, is a fine powder that had been previously spray-dried (any crystallinity in the native granule was destroyed by high-pressure steam). Based on intrinsic viscosity measurements performed at National Starch, $[\eta]_{0.5N\ NaOH} = 0.5$ dL/g compared with 0.9–0.95 dL/g for the untreated Hylon starch. The supplier estimates that the molecular weight of the EK. Fl. HY grade is $\sim 0.4 \times 10^6$ g/mol for the amylose fraction and ~ 10–25×10^6 g/mol for the amylopectin fraction.[36]

Film-grade EVOH, EVAL E 105A, was obtained from EVAL Co. of America (Lisle, IL). The EVOH contains 44 mol % ethylene, has a melt index of 12 at 210°C, and a number-average molecular weight, M_n, equal to 45,000. The weight-to-number average, M_w/M_n, is 2.22 (SEC, 90°C in dimethylacetamide/0.2% LiBr soln, polystyrene standard).[37] The peak melting temperature and glass transition are 165 and 55°C, respectively, for pure EVOH. Deionized water, glycerin, and naturally occurring triglyceride additives, used as plasticizers, lubricants, release agents, and melt-flow accelerators,[28] were provided through Warner-Lambert Co. (Morris Plains, NJ).

Blend Compounding

Three series of blends, containing different levels of each starch and EVOH, were compounded at the Novon Research Division of Warner-Lambert in Morris Plains, NJ.[30] Nomenclature, composition, and processing conditions are summarized in Table I. Ratios by weight of starch to EVOH for each series were 100 : 0, 85 : 15, 70 : 30, 60 : 40, 40 : 60, 50 : 50, 40 : 60, 30 : 70, 15 : 85, and 0 : 100. To aid in the processing of the starch fraction, a small amount of triglycerides was added to the dry mixture (3 parts to 100 parts starch). Dry materials (starch in powder form, EVOH in pellet form, and powder additive) were mixed in a 100 L Gral Mixer prior to extrusion blending.

Compounding of this experimental series of starch/EVOH blends took place in a Leistriz Standard Model-34, twin-screw, corotating extruder equipped with 10 separate zones. Feed was added to zone 1 through two ports. The dry mixture was fed, at rates of 10 to 20 kg/h, from a hopper directly above zone 1. A twin-screw outlet (for all powder blends) or a single screw (for the powder/pellet mixture) was employed to produce a constant feed throughput to the extruder. Glycerin was pumped through a liquid port at the at zone 2 at rates of 1.7–3.6 kg/h such that it was approximately 15 wt % of the total feed. In addition to the feed, deionized water was added through a separate port leading to zone 2 in amounts just necessary to prevent surging (by lowering the current draw) during the extrusion of certain blends. Surging is a phenomenon which occurs when there is a sudden transient rise in the current draw, usually as a result of material backing up in the feed zone or bridging in the feed hopper. At zone 8, a 200 mbar vacuum was applied for collection of volatiles (i.e., steam). The blends exited from zone 10 through the die at rates of 11–23 kg/h.

Processing conditions depended upon the composition of the blend. Peak extrusion temperatures (at zones 5 and 6) ranged from 165 to 190°C, except for the NC100 blend, for which lower temperatures and higher moisture levels were necessary for processing. Screw speeds ranged from 114 to 200 rpm. The blend consisting of only EVOH and glycerin was compounded on a Haake extruder (30 mm, $L/D = 13$). Peak extrusion temperature was 170°C, screw speed was 30 rpm, and throughput was 5.3 kg/h. All blends were pelletized upon exiting the extruder, cooled by air flow on a spiral conveyer, and collected and sealed in plastic bags.

Moisture and glycerin contents of the blends were determined after processing using titration and HPLC techniques, respectively. Further information on the processing and mechanical properties of selected blends has been published by George et al.[30]

Sample Preparation

Depending upon the characterization technique, blends were examined as extruded (pellet form), as pulverized (powder form), or after undergoing secondary processing (filament form). Pellets were pulverized for subsequent X-ray diffraction analysis using a Fritsch Pulverisette (Model 14701) cryogenic grinder with a 0.5 μm screen. Filaments were prepared by placing pellets in an Alex James One-Shot® fiber spinning apparatus, heating to 150°C, and extruding the blend through a spinnerette ($D = 0.03$ in. (763 μm), $L/D = 3$) at approximate shear rates of 40–140 s^{-1}.

Table I Model Starch–EVOH Blends[a]: Nomenclature, Composition, and Processing Parameters

Blend	Starch : EVOH by Weight	GLY Content (wt %)	Water Content (Wt %)	Max Extrusion Temperature (°C)	Screw Speed (rpm)	Output Flow Rate (kg/h)
High-amylose starch (Hylon VII) blends						
HY100	100 : 0	15.1	8.7	170	150	11.4
HY85	85 : 15	14.3	8.5	180	176	19.3
HY70	70 : 30	14.8	10.6	190	130	17.3
HY60	60 : 40	14.3	11.1	175	199	19.2
HY50	50 : 50	15.6	12.1	190	149	19.3
HY40	40 : 60	14.1	6.6	175	191	18.6
HY30	30 : 70	14.1	8.0	190	125	17.8
HY15	15 : 85	14.0	5.6	175	200	16.0
Native corn starch blends						
NC100	100 : 0	12.2	15.8	119	160	14.2
NC85	85 : 15	14.7	9.7	180	175	17.5
NC70	70 : 30	18.1	12.7	194	120	19.9
NC60	60 : 40	14.8	6.6	180	200	22.9
NC50	50 : 50	16.1	9.8	190	125	19.2
NC40	40 : 60	14.8	4.8	185	199	24.1
NC30	30 : 70	13.6	6.8	190	137	18.3
NC15	15 : 85	14.2	5.6	175	200	18.4
Waxy maize starch blends						
WM100	100 : 0	16.1	7.8	190	131	11.4
WM85	85 : 15	14.8	8.8	185	130	21.3
WM70	70 : 30	16.3	5.3	190	114	17.3
WM60	60 : 40	14.8	6.6	180	165	20.7
WM50	50 : 50	14.8	9.0	190	115	19.2
WM40	40 : 60	14.8	4.9	180	180	19.7
WM30	30 : 70	12.7	7.6	190	129	17.7
WM15	15 : 85	14.6	4.4	165	175	16.6
EVOH control						
EVOH/GLY	0 : 100	14.0	1.4	170	30	5.3

[a] Model blends containing starch were compounded using a Leistriz (34 mm) twin-screw extruder. The EVOH/GLY blend was compounded on a Haake (30 mm) extruder.

Because moisture content was found to vary depending upon the relative humidity (RH) at which the blend was stored, certain samples were conditioned by placing the pellets in closed chambers at room temperature and varying RH (produced from solutions of differing ratios of glycerin to water) for at least 1 week.[38] Humidity and temperature were recorded using a Testoterm 6100 thermohygrometer.

Methods of Characterization

Wide-angle X-ray Scattering

Wide-angle X-ray scattering (WAXS) patterns of blends were collected using a Rigaku automated standard powder diffractometer attached to a Rigaku RU 300 rotating anode generator with a copper anode assembly. A nickel beta filter was employed for all scans. The generator was operated at 50 kV and 200 mA. Powder from pulverized pellets were mounted on a glass slide by first making a suspension of the sample in collodion/amyl acetate, depositing the suspension on the slide, and allowing the liquid to evaporate. The glass slide was mounted in the diffractometer. A detector slit of 0.5°, scatter slit of 0.5°, and receiving slit of 0.3 were employed. Samples were scanned over the 2θ range from 2 to 50° (step size = 0.01°). The scan rate employed was fixed by the analysis sought: (1) 1° for determining accurate d-spacing determination, (2) 2° for estimating the degree of crystallinity, and (3) 10° for surveying a particular blend. The degree of crystallinity was estimated for the neat blends by using the crystallinity determination module in the Rigaku software which

employed Ruland's method.[39,40] Values of atomic and Compton scattering factors for the atoms composing each polymer were taken from the *International Tables of Crystallography.*[41]

Hot-stage WAXS was performed on a Rigaku RU 200 wide-angle powder diffractometer using the Rigaku high-temperature X-ray diffractometer attachment (Model CN231181). A scan rate of 2°/min was employed. Heating of the specimen took place in a nitrogen atmosphere, and ice water was used as the coolant system. Samples were heated at approximately 10°/min to fixed temperatures ranging from 20 to 230°C and remained at each temperature for the length of the scan (typically 20 min).

Thermal Analysis

Thermal analysis of the samples was performed under nitrogen using a Perkin-Elmer DSC-7 fitted with an Intracooler II. The DSC was calibrated using indium and zinc standards. High-pressure, stainless-steel capsules were employed to suppress volatile loss and sample degradation. Approximately 25 mg of material (cut pellets) was heated from −65 to 200°C, cooled to −65°C, and heated again to 230°C at a rate of 10°C/min for each trial. DSC trials were run after conditioning each sample at 50% RH or < 1% RH for at least 1 week. Titration was carried out concurrently with each DSC trial and a corresponding moisture content recorded for each sample.

Scanning Electron Microscopy (SEM)

Preparation of samples for SEM included fracturing filaments or pellets immediately after they had been immersed in liquid nitrogen for 1–5 min (depending on samples thickness). Surfaces were imaged as fractured or after etching out of the starch component. For etching, samples were placed in either aqueous solutions containing α-amylase (27 units/mg solid from *Asperillus oryzae,* Sigma Chemicals) or a control solution of distilled water. Both solutions were adjusted to a pH level of 6.9 using a sodium phosphate buffer (Sigma Chemicals). These solutions were heated at 37°C for 6 h. Samples were then rinsed with distilled water and allowed to dry overnight on filter paper. Samples were mounted on aluminum stubs with conductive tape and sputter-coated with gold palladium. A Cambridge Stereo-Scan scanning electron microscope was employed at a voltage of 10 keV. Images were recorded with Polaroid P/N 55 film.

Transmission Electron Microscopy (TEM)

Extrudates from the compounding process were microtomed to thicknesses below 1000 Å at temperatures from −20 to 15°C using a Reichert-Jung FC4E cryo-ultramicrotome. Prior to viewing in TEM, certain sections were placed in a stainer containing elemental iodine (Mallinckrodt Specialty Chemicals) and exposed to iodine vapor for 1 h to preferentially stain the amorphous starch-rich fraction. A JEOL 200 CX TEMSCAN electron microscope was employed at 200 keV to image the samples. Because of the sensitivity of both starch and EVOH to the electron beam, samples were imaged using low-dose techniques.[42] Images were obtained at relatively low magnification (5–10 kX) by first focusing on an area, translating to an adjacent area, and recording a 2–4 s exposure with Kodak SO-163 image plates. Details on this technique were given in a previous article.[34]

Moisture Content

Average moisture content of the samples was determined using a Mettler DL18 Karl Fischer titration system. Between 0.100 and 0.150 g of material was placed in a Mettler DO301 oven heated to a temperature of 200°C. Sample mass was recorded on a Mettler AE240 balance. Grade 5 dry nitrogen purge gas was passed through the oven at a rate of 200 mL/min and into the beaker containing reagent-grade methanol where titration takes place. Hydranol Composite 5 (Fischer Chemical) was used as the titrant. A period of 20 min from sample insertion in the oven to the time of titration occurred to permit sufficient vaporization of the moisture in the sample. After the automatic titration process was complete, a value for water content was recorded based on the initial sample mass.

RESULTS AND DISCUSSION

Our structural investigation of starch/EVOH blends was performed to gain insight into how well these materials will behave as biodegradable thermoplastics. First, the visible appearance of the blends after exiting the extruder and upon storage will give us an initial indication of the blend structure and stability of the blends from which to motivate more detailed studies (e.g.: Do chemical reactions as evident by color changes occur? Does melt fracture, swelling, or foaming of the extrudate take place? Are the blends opaque, indicating crystallization and/or phase separation? Are the blends at equilibrium? Do the materials change in opacity as a func-

Table II Appearance and Flexibility of the Model Blends

Blend	Color	Clarity	Texture	Foaming	Flexibility (180° Bend)
High-amylose starch (Hylon VII) blends					
HY100	Amber	Translucent	Melt Fracture	No	No, split occurs
HY85	Amber	Translucent	Smooth	No	No, split occurs
HY70	Yellow	Translucent	Smooth	No	Yes
HY60	Yellow	Translucent	Smooth	No	Yes
HY50	Yellow	Translucent	Smooth	No	Yes
HY40	Yellow	Translucent	Smooth	No	Yes
HY30	White	Translucent	Smooth	No	Yes
HY15	White	Translucent	Smooth	No	Yes
Native corn starch blends					
NC100	Yellow	Translucent	Smooth	No	Yes
NC85	Yellow	Translucent	Smooth	No	Yes
NC70	Yellow/white	Translucent	Mostly smooth	No	Yes
NC60	Yellow/white	Translucent	Smooth	No	Yes
NC50	White/yellow	Opaque	Smooth	No	Yes
NC40	White/yellow	Opaque	Smooth	No	Yes
NC30	White	Opaque	Smooth	Slight	Cracks on surface
NC15	White	Opaque	Smooth	No	Yes
Waxy Maize starch blends					
WM100	Clear	Translucent	Melt Fracture	No	No, Brittle
WM85	Clear	Translucent	Melt Fracture	No	No
WM70	Clear	Translucent	Melt Fracture	No	Split occurs
WM60	White	Translucent	Melt Fracture	No	Yes
WM50	White	Opaque	Melt Fracture	Yes	Yes
WM40	White	Opaque	Melt Fracture	No	Yes
WM30	White	Opaque	Melt Fracture	Yes	Yes
WM15	White	Opaque	Melt Fracture	No	Yes
EVOH control					
EVOH/GLY	White	Opaque	Smooth	Smooth	Yes

tion of storage condition and time? Does plasticizer leach out of the pellets?). Next, wide-angle X-ray scattering (WAXS) is performed to discern the crystalline phase types occurring in each blend, if physical aging occurs (such as through retrogradation of the starch fraction) and if crystalline shifts occur as a function of temperature. (The use of flat film WAXS to explore orientation effects is presented in a separate article on fiber spinning.[33] No orientation was observed for the extrudate and filament samples employed in this study.) Through the use of DSC, the thermal behavior of the blends can be analyzed for glass transitions, melting/crystallization behavior, and indications of miscibility. Examination of the blends with SEM allows us to determine if micron scale phase separation is occurring through observations of blend surfaces as fractured or enzymatically etched. Once the effectiveness of SEM is determined for observing the morphology of certain starch/EVOH blends, orientation of phase domains as a function of shear (in capillary flow) can be established as well as the stability of the blend structure in the melt. Finally, TEM is a useful technique for understanding differences in phase separation between different starch varieties with EVOH since submicron details can be explored. By combining information attainable with these structural characterization techniques, we can then predict and explain results from processability and property tests (e.g., fiber spinning results, mechanical behavior of the blends, and biodegradation rates).

Observation of Extrudate (Pellets) After Compounding

Observations of the appearance and flexibility of the model blends are listed in Table II. The blends containing amylose were deep amber or yellow in color, indicating that certain degradation and Maillard

browning reactions had occurred.[43-45] The WM100 blend appeared clear, indicating that such reactions were not prevalent in this system. As the EVOH content was increased, the materials appeared whiter and more opaque, suggesting phase separation and crystallization of the synthetic component. Exposure to a saturated water atmosphere turned pellets from all blends opaque, except for the HY100, HY85, and NC100 blends. Pure EVOH does not take up significant moisture (<3%) and remains clear when saturated with water; however, the EVOH/GLY control sample becomes opaque and absorbs up to 8% moisture.[46] This increase in moisture level may enhance the refractive index difference between crystalline domains (which exclude plasticizer) and amorphous domains (which with glycerin is known to absorb water), making the EVOH/GLY blend appear opaque. Similar behavior is believed to occur in the starch/EVOH blends.

Surface observation of the WM100 and HY100 extrudates showed irregularities which may be due to melt fracture.[47] Melt fracture is a phenomenon associated with the elastic instability of a polymer to flow and is usually associated with shear stresses above 10^5 Pa.[48] It was not observed in the NC100 material, which is probably due to the high level of moisture present (thus lower shear) during the compounding of this particular blend. Melt fracture was apparent in all of the WM blends and was probably due the level of branching and lower amount of entanglements in this starch component. However, none of the NC or HY blends with EVOH showed evidence of melt fracture upon exiting the extruder.

Visible foaming at the die was generally not a problem since conditions were optimized to eliminate this phenomenon. Conditions to suppress foaming included lowering the amount of water injected into the extruder and replacing it with a fixed amount of glycerin, a lower vapor-pressure component; venting of water vapor from the extruder's two zones before reaching the die; and setting the temperature at the die from 90 to 95°C, which is lower than the boiling temperature of water at atmospheric pressure (glycerin was not expected to contribute to the foaming process since its boiling point is 290°C). Despite these efforts, a small amount of foaming was observed in certain blends (i.e., NC30, WM50, and WM70).

A viscous fluid was observed to migrate to the surface of some pellets as they were stored. The composition of the fluid is believed to be mainly glycerin from its consistency and from the fact that it has a lower vapor pressure than that of water, thus making it less likely to evaporate from the surface. Blends exhibiting this coating were generally high in EVOH content, greater than 70% for the WM and NC starch blends. The fluid was also observed on the surface of all the HY blends. These observations seem to indicate that the partitioning coefficient for glycerin and water was higher for blends containing amylopectin than those containing amylose or EVOH. It may also mean that glycerin and/or water was excluded from the crystalline domains of EVOH or amylose complexes, thus lowering the apparent partitioning coefficient for these domains. Measurements of the glycerin content via HPLC did not show a significant drop in plasticizer levels for the blends higher in EVOH content; however, values for the bulk glycerin content may be biased due to the glycerin on the surface of the pellets.[30]

Wide-angle X-ray Scattering

Wide-angle X-ray scattering (WAXS) provides information about the short-range order of the molecular constituents in polymer blends; levels and types of crystallinity can be determined by this technique. WAXS of starches has been often used to classify starch by their distinct powder patterns (e.g., A, B, and C types of native starches).[49-51] When starch is thermally, chemically, or mechanically treated, it often exhibits the "V"-type pattern, which is formed upon complexing of amylose or amylopectin with varying agents (usually nonpolar molecules which insert themselves within the interior of the polymer helices).[50] Thus, WAXS can be used to track morphological changes in starch as it has been extruded under varied heat, shear, and moisture levels,[52,53] as a function of aging, and, with the use of a hot stage, after heating to various temperatures.

Crystalline Phase Types

Blends were first surveyed after compounding to determine the crystalline phase types that existed after initial processing. WAXS scans of representative compositions of the three types of starch blends, taken at a scan rate of 2θ of 10°/min, are shown in Figure 1. Peaks associated with the EVOH component were evident at 2θ equal to 10.8, 20.4, and 21.7. These results indicate that a portion of the EVOH fraction was forming a distinct crystalline phase for which the melting points as determined by DSC occur over the range 120–150°C. The level of crystallinity measured via WAXS is estimated to be 16 ± 3% for the EVOH/GLY control sample. For blends containing starch, the estimation of crystallinity levels via WAXS using Ruland's method[39] is

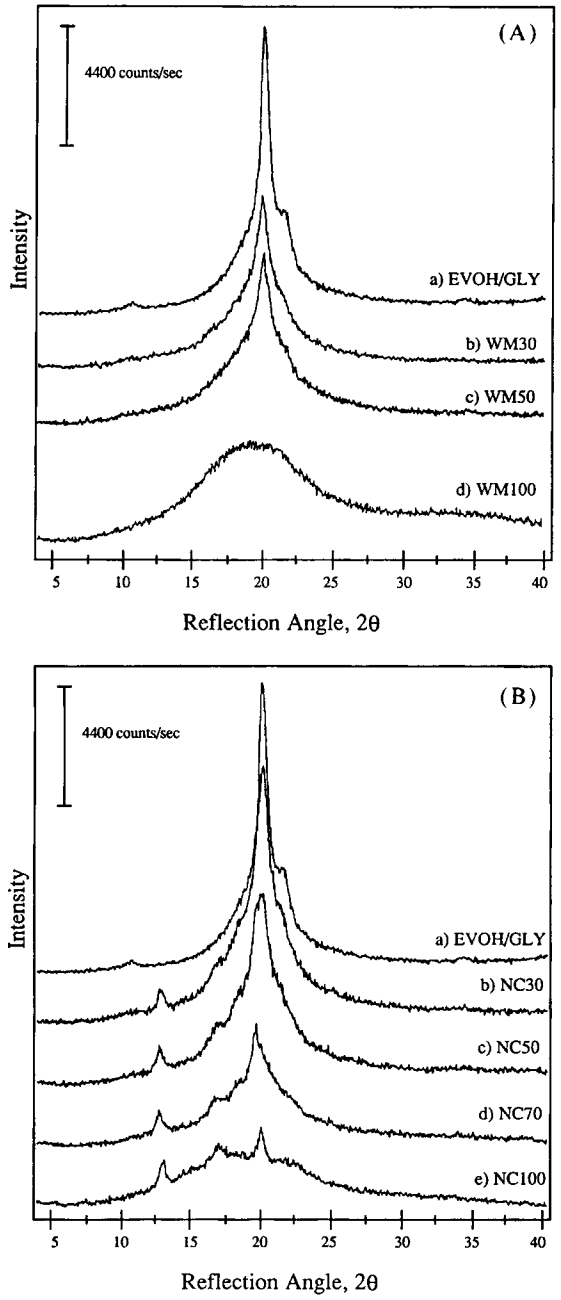

Figure 1 (A) Wide-angle X-ray powder diffraction spectra for selected WM blends compared with the EVOH control: (a) EVOH/GLY; (b) WM30; (c) WM50; (d) WM100. (B) Wide-angle X-ray powder diffraction spectra for selected NC blends compared with the EVOH control: (a) EVOH/GLY; (b) NC30; (c) NC50; (d) NC70; (e) NC100. (C) Wide-angle X-ray powder diffraction spectra for selected HY blends compared with the EVOH control: (a) EVOH/GLY; (b) HY30; (c) HY50; (d) HY100.

more difficult since some of the peaks corresponding to the amylose complex overlap with the EVOH peaks. Scattering associated with the EVOH crystalline phase became less apparent, expectedly, as the starch content is increased. The WM blends, which contain only amylopectin, did not show crystallinity associated with the starch fraction [Fig. 1(A)]. For the blends containing amylose, crystallinity associated with the starch fraction was apparent from peaks occurring at 12.9, 16.6, 18.3, 19.7, and 22.4° for the HY VII and NC starch blends [Fig. 1(B) and (C)]. To help understand the changes which occurred in the structure of the starch fraction during the extrusion blending process, the results of WAXS scans taken of the raw starch materials are shown in Figure 2. The NC and WM raw starches yielded WAXS patterns that are representative of the "A"-type pattern documented in the literature.[54-56] These patterns also indicated that these starches existed in granular form and that the amylopectin fraction is responsible for most of the sample's crystallinity. The HY starch exhibited a WAXS spectrum typical of a completely amorphous polymer. This is consistent with the fact that the HY starch granules had been steam-treated and all crystallinity was destroyed prior to compounding.

The WAXS spectra of the neat starch blends are shown in Figure 3; the scan of the triglyceride additives is also shown in this figure for comparison. After compounding the starch with glycerin, water, and the triglyceride additives at high temperature (as listed in Table I), scans taken of these materials exhibited markedly different structures. The WM starch, which was initially highly crystalline, exhibited only amorphous scattering. Conversely, the HY starch, initially amorphous, exhibited peaks asso-

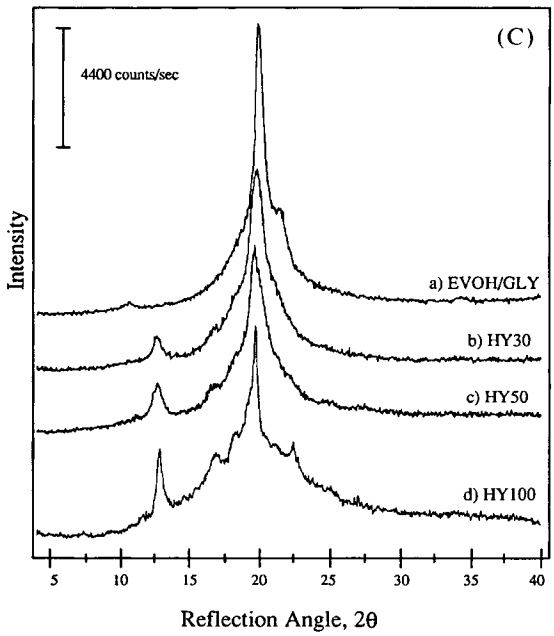

Figure 1 (*Continued*)

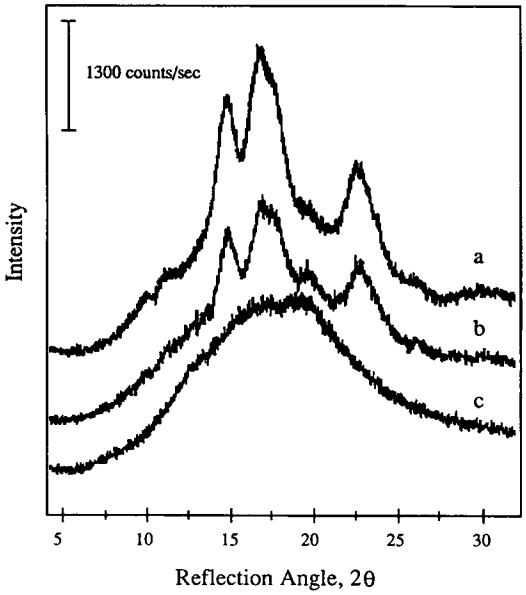

Figure 2 Wide-angle X-ray diffraction spectra for the starches before compounding: (a) Amioca WM; (b) Melojel NC; (c) EK Fl. HY.

ciated with a crystalline component. The peaks at 2θ equal to 12.9, 16.6, 18.3, 19.7, and 22.4° can be attributed to the amylose complex which forms between the linear starch fraction and certain fatty acids and triglycerides which also occur naturally in the starch granule.[50] The estimated crystallinity for the HY100 blend was 10 ± 2%. These peaks did not correspond to scattering from the triglyceride additives (peaks of which are measured at 5.7, 19.3, 21.0, and 23.2); however, from DSC data, it is hypothesized that at least one of the additives may have formed complexes with the amylose fraction (in addition to the complex formation that occurs between lipids naturally present in the starch granule[57]). The NC blend series also showed peaks at similar angles, indicating the formation of similar amylose complexes. The ratio of the peak areas in the NC100 sample to its amorphous scattering was less than that observed for the HY100 material; hence, crystallinity is less than 5% for this material. Finally, the WM starch blends, in which the WM component initially showed an A-type crystalline pattern, exhibited essentially no crystallinity; only a broad region of amorphous scattering was observed. Again, peaks associated with the triglyceride additive were not visible from the WAXS scans. Overall, these results indicated that the amylose formed a second distinct crystalline phase in the starch/EVOH blends through complexation and that essentially all of the branched amylopectin fraction remained amorphous after thermomechanical processing.

Physical Aging Studies

To discern if certain changes occur in the level and/or type of crystallinity as a function of time, WAXS of newly compounded blends and blends which were allowed to age over time were collected. Results of scans taken for blends after 1 week indicate only a slight increase in starch crystallinity for the NC and HY series; otherwise, no noticeable difference in the spectra is observed. Patterns remain relatively constant for powder samples which were tested after 6 months and 1 year after compounding and appear similar to those in Figure 1. It should be noted that the as-processed moisture content was maintained by storing samples in several layers of polyethylene and foil wrapping and that variations in the spectra are not due to fluctuations in water content.

WM blends have been documented in the literature to undergo crystallization over time. This retrogradation phenomenon is thought to be responsible for the staling of bread.[58] Usually, the crystallization of amylopectin is facilitated by the presence of water in amounts greater than 14%. A slight 2θ peak has been measured around 20° by others for WM gels that have been aged over a period of days to weeks. Wide-angle X-ray diffraction measurements for the WM100 blend (with ~ 8% moisture) do not show evidence of a peak that is discernible

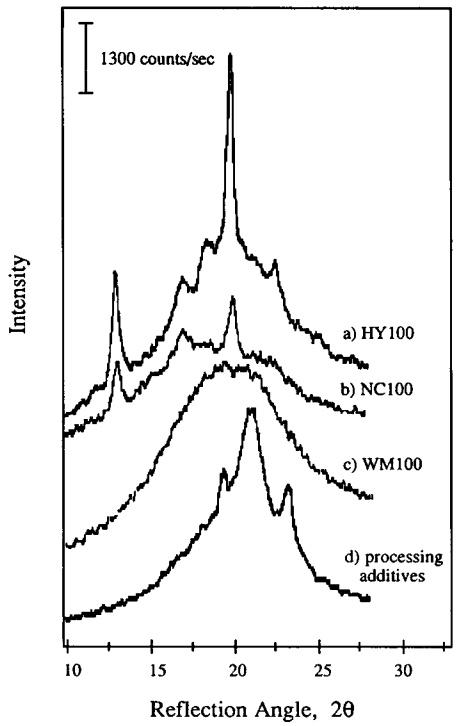

Figure 3 Wide-angle X-ray diffraction spectra for the (a) HY100 blend, (b) NC100 blend, (c) WM100 blend, and (d) processing additives.

from the background scatter, even after 2 years of aging. Patterns taken are similar to those in Figures 1(a) and 3.

Temperature Dependence of WAXS

To complement the DSC analysis and detect transitions attributed to the crystalline fraction of the starch in the blends, WAXS was performed on the HY100 blend at various temperatures. Pulverized pellets of the HY100 blend were mounted on glass slides and heated to various temperatures at rates of approximately 10°C/min. Signal was monitored at 2θ equal to 20.8° during the heating cycle to determine if significant shifts in intensity occurred. When the desired temperature was attained, the temperature ramping cycle was stopped and a WAXS scan was taken over a period of 15–20 min (see Figs. 4 and 5). One should note also the decrease in signal from data shown in previous figures. The signal-to-noise levels are lower due to the hardware of the hot-stage attachment (i.e., beryllium windows, platinum heater).

The first trial consisted of taking a scan at 20°C (slightly below room temperature due to the coolant), heating to 60°C, taking a scan, then cooling the sample down to room temperature (25°C) and taking a new scan. Results are shown in Figure 4. There is a noticeable increase in the scattering intensity of the crystalline peaks, which must indicate

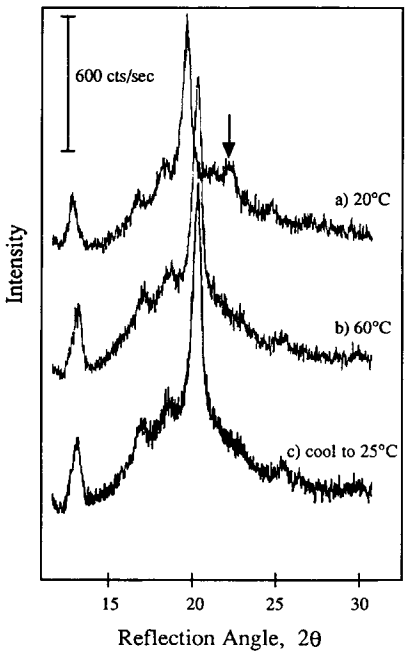

Figure 4 Wide-angle diffraction spectra of the HY100 blend taken at (a) 20°C, (b) at 60°C, and (c) after cooling to 25°C. Note the disappearance of the peak at 22.5°.

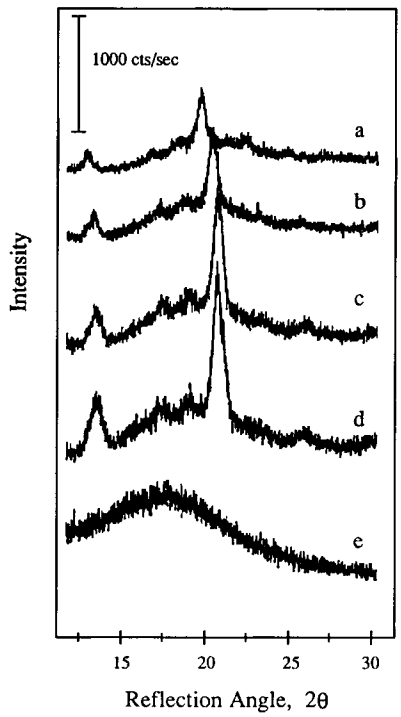

Figure 5 Wide-angle X-ray diffraction spectra taken isothermally at various temperatures for an HY100 powder sample: (a) 20°C; (b) 60°C; (c) 100°C; (d) 150°C; (e) 230°C.

a shifting to a higher level of crystallinity (i.e., annealing at 60°C) and an overall decrease in the chain-to-chain lateral spacing within the amylose crystallite. The initial scan at 20°C corresponded closely with values for 2θ taken for the V-type patterns recorded by Mercier and others.[52,59,60] The shifting in the scattering peak angles represent a shifting in the spectra from a hydrated form to a dry form of the V-complex. This increase in peak intensity and level of order can also be attributed to a decrease in the moisture level of the sample that results from drying of the sample over the course of heating.[61] The shift from the hydrated form to the dried form of the V-amylose complex represents shifts in the seven residue left helical packing of 1.38 to 1.31 nm between helices.[52] The disappearance of a small peak at 2θ equal to 22.4° also occurs upon heating the sample to 60°C; this peak could possibly be attributed to melting of any crystallized starch which would produce an A or B crystal type.[62–64]

A second experiment was undertaken in which the HY100 sample was heated from 20°C to various temperatures (60, 100, 150, and 230°C) at which the isothermal scans were taken (see Fig. 5). Again, an increase in the scattering intensity for each WAXS spectra was observed due to drying of the starch sample. A shift to a higher scattering angle was ob-

served, even to a higher angle in the 100 and 150°C cases from that of a 60°C trial. This behavior seemed to indicate that the sample was drying out, forming a more closed packed crystal. The crystalline scattering peaks associated with the amylose complex exist until 230°C. It was at this point that the sample completely degraded and the crystalline pattern was no longer visible (i.e., V-amylose melting occurs near the degradation point of the sample).

Thermal Analysis

In the previous section, EVOH, amylose, and amylopectin are shown to be semi-crystalline to different degrees. Differential scanning calorimetry was employed to discern thermal transitions (e.g., melting, crystallization, glass transitions) and to gain some information on the miscibility between starch and EVOH. As described in the experimental section, three scans for each sample were performed. Since plasticizers, especially water, will migrate out of the sample during heating, the first heat values for melting temperature will give the best indication of the influence of the plasticizers on the melting point and glass transition for the blend. Cooling and second heating cycles provide more information on reversible transitions by erasing any prior thermal histories associated with the sample.

A typical heat/cool/heat cycle is shown in Figure 6 for an NC70 blend (mass = 20.86 mg) conditioned in a 50% relative humidity chamber. The moisture content of this sample was measured to be 5.0%. In the first heat, a small endothermic peak (ΔH = 0.8 J/g) was observed at an onset temperature of 56°C with a peak at 60.5°C. A second endotherm associated with the melting of EVOH crystallites occurred with an onset temperature of 121.5°C and a peak temperature of 133°C (ΔH = 10.8 J/g). A shift in the heating curve, associated with the glass transition of starch, was not readily apparent in this scan. It may have been obscured by the base line or the smaller endothermic transition. After 2 min of holding at 200°C, the cooling cycle was started. At the scan rate of −10°C/min, crystallization of the EVOH occurred at an onset temperature of 98.5°C and a peak temperature of 94°C. The enthalpy of transition for the EVOH crystallization was 9.9 J/g. The smaller, low-temperature, endotherm was again apparent in this blend with an onset temperature of 38°C and a peak temperature of 35°C (ΔH = 0.74 J/g). After holding for 2 min at −65°C, the sample was reheated. In the second heating cycle, transitions similar to the first heat were observed, although slightly shifted in temperature. For the small endotherm, the onset occurred at 48°C with

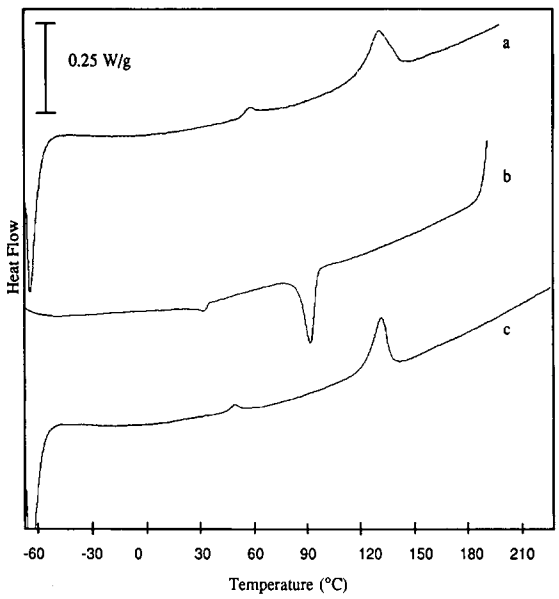

Figure 6 DSC curves for (a) first heating, (b) cooling, and (c) second heating cycles for the NC70 blend. Scan rates were 10°C/min. Sample was conditioned to 50% RH before testing.

a peak at 52°C, which was lower than the measured temperature in the first heating cycle. The EVOH melting transition began at 125°C and peaked at 134°C. This endotherm is much sharper than in the first heat and was slightly shifted to a higher temperature, implying a more narrow distribution of somewhat larger crystal sizes and melting within a purer phase. Overall, the enthalpies associated with both transitions were lower than those values measured from the first heat. The EVOH peak has a ΔH equal to 8.5 J/g, and, for the lower temperature transition, ΔH equals 0.7 J/g. These two transitions were observed in every blend which contained both starch and EVOH. Further cooling and heating cycles yielded reproducible results.

DSC results for the series of blends are shown in Figures 7–10. Each blend was conditioned for at least 1 week at 50% RH; moisture and glycerin contents for each component are shown in Figure 11 (a linear relationship with starch content is evident). In Figures 7 and 8, values for temperature and enthalpy are given for the lower-temperature transition. To clarify the discussion, the term "S-transition" will be used to designate this transition since it is only present in DSC scans taken with blends containing starch. This transition occurred over the range of 40–65°C. In Figures 9 and 10, the endotherm corresponding to the melting of the EVOH component is presented. The normalized enthalpy of this transition was determined in order to roughly estimate the percentage of the EVOH component which had

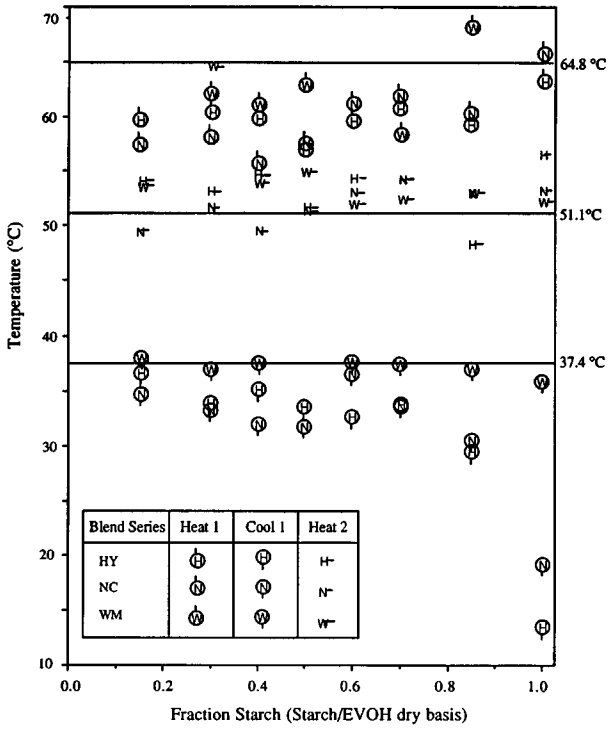

Figure 7 Peak S transition temperatures as measured by DSC for the heating/cooling/heating cycles of the HY, NC, and WM model blends which were conditioned to 50% RH. Values on the right of the graph correspond to peak transition temperatures for the neat triglyceride additives.

crystallized. For blends containing EVOH, the heating runs yielded endotherms which correspond to the melting of EVOH crystals. Peak temperatures ranged from 120 to 152°C depending upon composition and storage conditions. Smaller multiple transitions were also observed in these systems that were extremely dependent on moisture content. These transitions are most likely related to the glass transition of the starch and EVOH, but the transitions often overlapped with the S-transition. For this reason and because of the low signal-to-noise level of the glass transition, we do not attempt to quantitatively describe these data here.

The S Transition

The S transition ($\Delta H < 4$ J/g) that occurs between 50 and 70°C may be attributed to any of a number of factors which include melting of the amylopectin fraction,[65] amylose-complex melting due to plasticizer effects, glass transition as influenced by physical aging,[66] and, perhaps, crystallization of the processing additives. The disappearance of a small WAXS peak near 60°C in the HY100 at 2θ of $\sim$ 22.5° may suggest melting of a retrograded starch that yields an A or B X-ray diffraction pattern.[64] Hot-stage WAXS showed that amylose-complex melting occurred at temperatures above 200°C, which is much higher than the measured S-transition. Peak temperatures for the heating/cooling/heating cycles for the starch/EVOH blends are displayed in Figure 7. DSC of the triglyceride additives yielded reproducible melting transitions that occurred in the range from 42 to 65°C. Values obtained for the first heat, cooling, and second heat are represented by lines drawn across the composition range. The first heat transition was slightly lower than that measured for the neat triglyceride additive. The cooling and second heating cycle yielded values for temperature that roughly approximated that of the pure triglycerides. We can thus conclude that the S transition observed in this temperature range is primarily due to the additive.

A note should be made, however, regarding the enthalpy of these transitions. Figure 8 displays the enthalpy associated with the S transition for the series of starch blends (values from the first heating cycle are connected by lines). Overall, the enthalpy determined from the cooling and second heating cycle was similar and increased, as expected, nearly linearly with triglyceride composition. In the first heating cycle, however, the enthalpy of transition increased at a greater rate as the starch content increased for the NC and WM blends. In addition, the

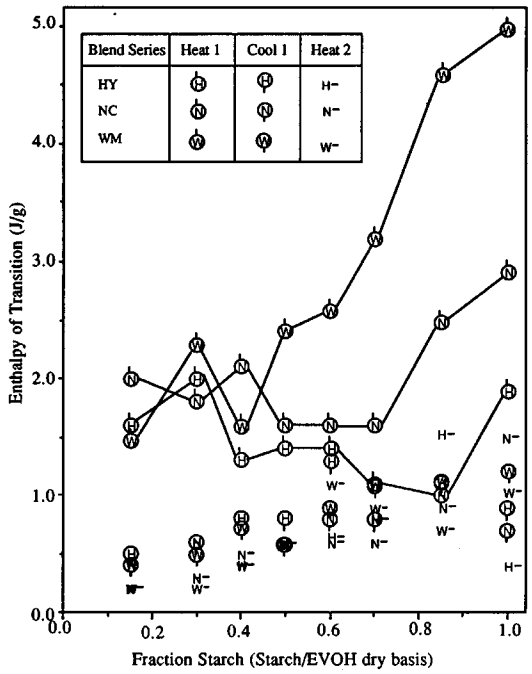

Figure 8 Enthalpy of the S transition for the HY, NC, and WM model blends which were conditioned to 50% RH.

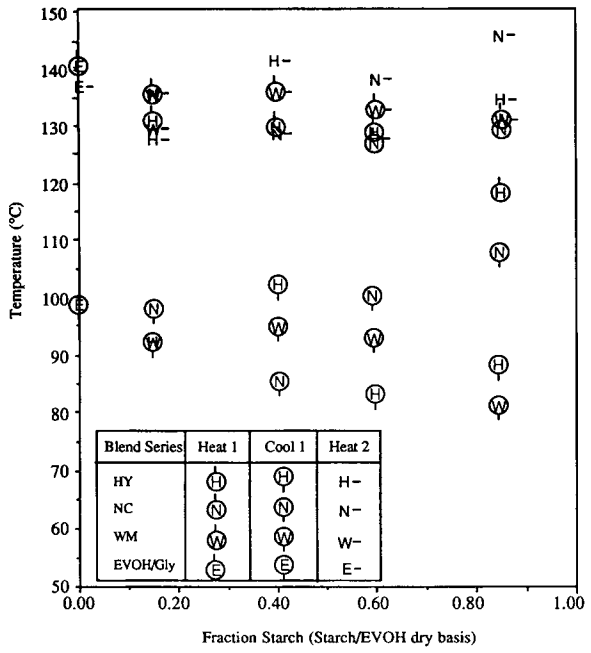

Figure 9 Peak EVOH transition temperatures for the heating/cooling/heating cycles of the HY, NC, and WM series of model blends which were conditioned at 50% RH. Values for Heat 1 and Heat 2 represent melting transitions. Values for Cool 1 represents EVOH crystallization.

enthalpy of this transition for the first heat was also much higher than in the cooling and second heating cycles for all of the starch blends (i.e., all of the S transition in the first heat cannot be due to triglyceride alone). This difference suggests that the lower-temperature endotherm between 55 and 60°C is partially due to the "melting" of retrograded starch.

EVOH Crystallization

From WAXS, it was shown that the EVOH component in the starch blends crystallized. Since the glass transitions of both starch and EVOH components are hard to distinguish from DSC, we turned our attention to the EVOH melting/crystallization transition in order to gain information on the miscibility of these components (i.e., an increase in melt miscibility will lead to a depression in the melting point). The effect of starch type on the crystallization behavior of the EVOH component is shown in Figure 9, which shows the peak melting temperature for the heating/cooling/heating cycles for each blend conditioned to 50% RH. Overall, the EVOH melting points in the HY and NC starch blends generally occurred at lower temperatures, possibly indicating increased miscibility in the melt between the amylose-containing starch types with EVOH.

DSC measurements have shown that the melting point of EVOH decreases as the amount of starch in a blend is increased. Usually, this depression will provide evidence for melt miscibility; however, up to 30% of the total blend consists of glycerin and water plasticizers which can both act to depress the melting point of the EVOH component. To estimate the effect of the plasticizers on the melting-point depression, the following comparison is made: First, values for moisture and glycerin content for the three-blend series are shown in Figure 11. Overall, the glycerin content is relatively constant among the blends (~ 15 wt %). The addition of glycerin causes about a 15°C decrease in the crystallization temperature of EVOH (from 165°C to approximately 150°C). Since the glycerin level in the blends is relatively constant, the melting point should stay relatively constant for the blends if starch and EVOH are completely immiscible in the melt (assuming uniform partitioning of plasticizer between the respective types of polymer domains). At 50% RH, the amount of moisture contained in each of the starch varieties is relatively constant, but increases with starch content (from 3 to 8%). Since melting points follow an inverse behavior with plasticizer content, one might assume that the melting-point depression is due solely to increased levels of water. However, in Figure 12, the peak melting temperatures for the EVOH melting transition (first heat) and corresponding moisture contents are

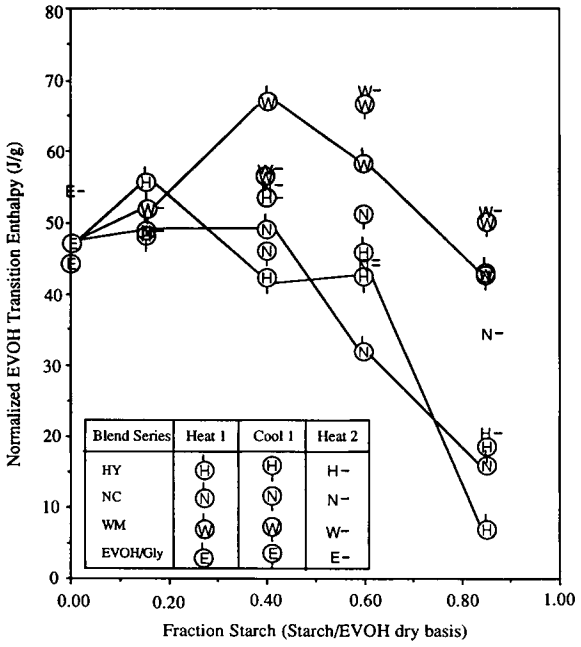

Figure 10 Normalized EVOH transition enthalpy for the heating/cooling/heating cycles of the model blends.

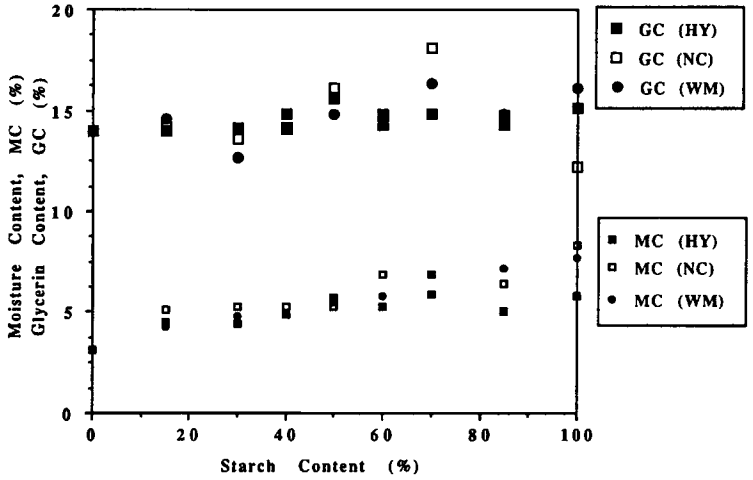

Figure 11 GLY and moisture contents for the NC series of blends after conditioning to 50% RH for 1 week.

shown at 50% RH and 0.5% RH. (At 0.5% RH, the blends contain less than 2% moisture and moisture content does not increase with starch content.) At both humidity levels, the blends show an approximately 10° decrease in peak melting temperatures

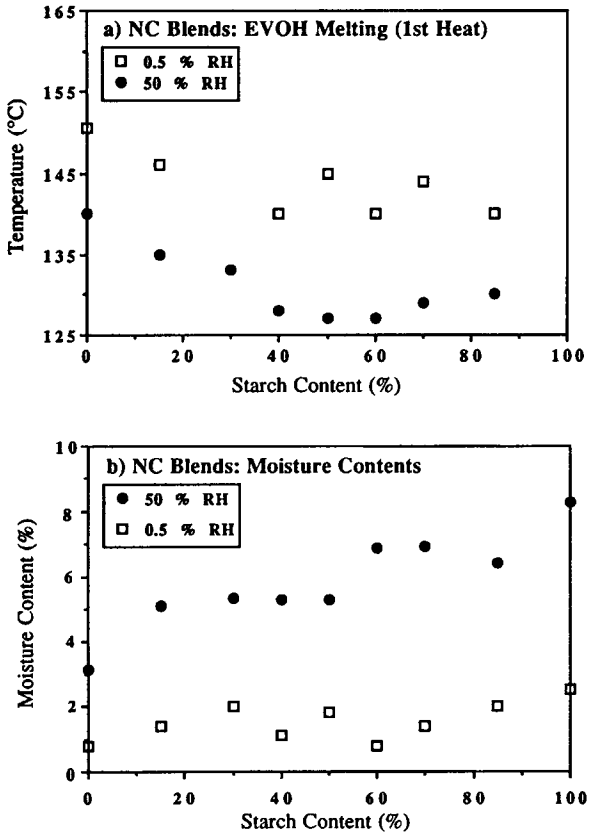

Figure 12 (a) Peak melting temperatures of EVOH and (b) moisture contents for the NC blends after conditioning at 0.5 and 50% RH for 1 week (DSC first heat cycle).

over the composition range of 0–85% starch. The difference in melting points ranges from 10 to 15°C and is a linear function of the increase in moisture levels at higher relative humidity. Thus, from DSC measurements of the blends, about 10°C depression in the melting point of EVOH is attributable to glycerin and from 10 to 15°C depression in the melting point at 50% RH is due to the water in the starch/EVOH blends (note: the presence of glycerin increases the water uptake of the EVOH component). The presence of WM starch leads to less than a 5°C depression, NC starch, up to 10°C, and the HY starch, up to 15°C for the blends at 50% RH. Thus, miscibility *does* increase as the amylose content in the starch blends increases. Although temperatures from the second and third scans in DSC, in most cases, yield more accurate information since the thermal histories of each blend are made constant, migration of glycerin and water within and out of the blends may cause significant changes in the temperature of crystallization and melting (up to 25°C). Thus, values for first heat are the most reliable and tell us the most information about the blend.

The transition enthalpy, normalized to the amount of EVOH in the blend in order to assess crystallinity levels, is plotted in Figure 10 as a function of starch content. If there is no effect on the level of crystallization of the starch or plasticizers, the values for normalized transition enthalpy should be constant. Values for the first heat (connected dots) show an increase in EVOH crystallinity up to 40% starch content. This behavior was not as dramatic for the second heating and cooling cycles and is probably a result of the initial thermal history of the blend during compounding and storage. Crys-

tallinity subsequently dropped off at starch contents above 50% for the HY and NC blends as is evident in all of the heating and cooling cycles. Higher transition temperatures and values of enthalpy may indicate increased phase separation between the starch and EVOH components; the purer the EVOH phase, the more it will crystallize. Overall, the WM blends showed the highest transition temperatures and transition enthalpies, indicating that the two polymer components are well phase-separated. DSC results for the NC and HY blends seem to indicate that there is some miscibility between the starch and EVOH in the HY and NC blends.

Electron Microscopy Studies

SEM of Untreated Fracture Surfaces

Electron microscopy was next performed to obtain information on the phase morphology of the starch/EVOH blends. First, the untreated fracture surfaces were examined with scanning electron microscopy (SEM). Representative blend fracture surfaces for the WM50, NC50, and HY50 blends are shown in Figure 13. SEM showed no evidence of the original WM or NC starch granules such as are evident in thermoplastics employing starch as a filler.[67-69] Brittle fracture bands were visible in all blends. Starch-rich or EVOH-rich domains were not directly evident on the fracture surfaces. Small tufts (< 0.2 μm), visible on the NC50 sample, are indicative of some ductility prior to fracture. These regions appear bright in the micrographs due to charging of the specimen. Some small voids (< 0.5 μm) were evident in the WM, NC, and HY blends; these may be attributed to a small amount of foaming during the processing of the blends.

Overall, examination of the fracture surface does not lead to much insight into the phase behavior of the particular blends. Because no distinct phases were evident, one might propose that there is considerable miscibility between the sample phases. However, similarities in the mechanical properties of the EVOH and starch components at low temperature will yield similar fracture behavior even for completely incompatible materials. In addition, there appears to be good interfacial adhesion between the polymer components. Finally, since the glass transition of the both components is probably near or above room temperature, a relaxation of a more "rubbery" component (as the sample heats up to room temperature after cryofast fracture) that would provide a distinction between the rubbery and plastic domains, does not occur.[70]

Blend Morphology as Observed by SEM and TEM

To distinguish between starch- and EVOH-rich domains, etching away of one component or preferential staining is necessary. In the SEM study, enzymatic etching[71] was employed according to the procedure outlined in the experimental section. The α-amylase enzyme attacks the $\alpha(1,4)$-glycosidic linkage in both amylose and amylopectin, facilitating their removal from the blend structure into an aqueous solution. For TEM imaging, iodine vapor is used to provide the required levels of contrast to discern starch-rich domains from EVOH-rich areas. Both techniques yielded useful information about the blend morphology of the starch/EVOH blends.

SEM micrographs of untreated and etched surfaces of WM70 filaments are shown in Figure 14. In Figure 14(a), an untreated WM70 showed evidence of small voids, probably due to foaming during processing. In Figure 14(b), the etched WM70 filaments exhibited significant removal of the starch-rich fraction. The volume removed, as determined by image analysis, was less than 70%, however, since some of the WM was encapsulated (even at this composition) and was therefore not accessible to the etchant. (Note that weight loss determination of volume removal was not possible due to unknown partitioning of the water and glycerin components after the etching procedure.)

Results of etching filaments of representative WM, NC, and HY blends are shown in Figures 15, 16, and 17, respectively. The morphology of the WM blends was most effectively revealed by etching. In Figure 15(a), the etched WM30 blend exhibited approximately spherical cavities which ranged in size from 0.1 to 4 μm. In some areas, smaller domains in the process of coalescing were observed. Slightly smaller, yet more numerous, domains were visible in the WM50 sample. These domains ranged in size from 0.05 to 3 μm in size and were shaped like prolate spheroids. In both cases, the EVOH component seemed to compose most of the matrix structure of the blend.

More extensive removal of the starch-rich domains was observed for the case of the WM70 sample [Fig. 15(b)]. Because starch was the majority component in this blend, one would have expected complete collapse of the filament which has been etched. Due to incomplete etching, one can conclude that this partial removal is that of accessible starch-rich domains and that the EVOH-rich domains contribute to most of the matrix of this particular blend and may even encompass large starch-rich domains. Fibril-like threads approximately 0.4–0.7 μm in di-

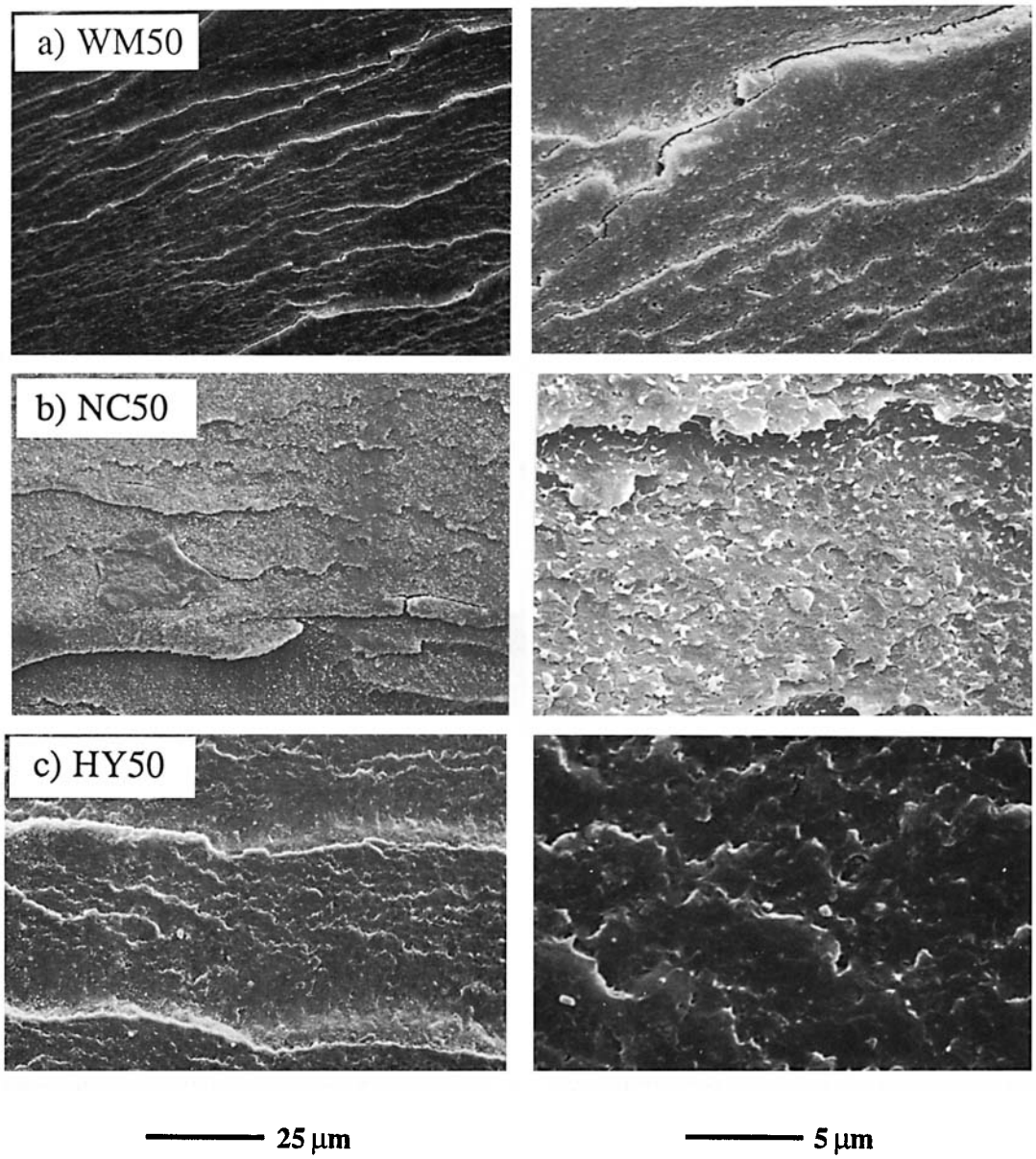

Figure 13 Scanning electron micrographs of cryofracture surfaces for the (a) WM50, (b) NC50, and (c) HY50 extrudates. Images on the right side represent magnified views of the surfaces on the left. Distinct phase domains are not evident using this method.

ameter were visible on the etched surface and appeared to be intertwined among each other and the remaining unetched bulk sample. It should be noted that these fibrils form during flow through the capillary and would therefore be oriented predominantly along the longitudinal direction of the filament. Fibrils observed in this axial cross-sectional view have most likely folded over upon drying of the etched filament. These observations led us to propose that a co-continuous morphology forms at this composition since the EVOH-rich domains were distributed throughout the blend structure even though EVOH was the minority component. The fact that the EVOH domains appeared as fibrils indicates that there has been a significant amount of orientation within the melt as it passed through the spinnerette which became quenched in as the filament cooled.

In Figure 15(d), the result of etching the WM85 filament is shown. In this case, the filament collapsed during the etching treatment. EVOH-rich fibrils approximately 0.35 μm in diameter and of lengths greater than 5 μm remain after etching. At this composition, the starch-rich phase formed a matrix in which the minority EVOH component experienced extensive orientation in the WM85 blend during capillary flow through the spinnerette.

Etching of the NC starch blends was less effective. Removal of the starch-rich domains was apparent

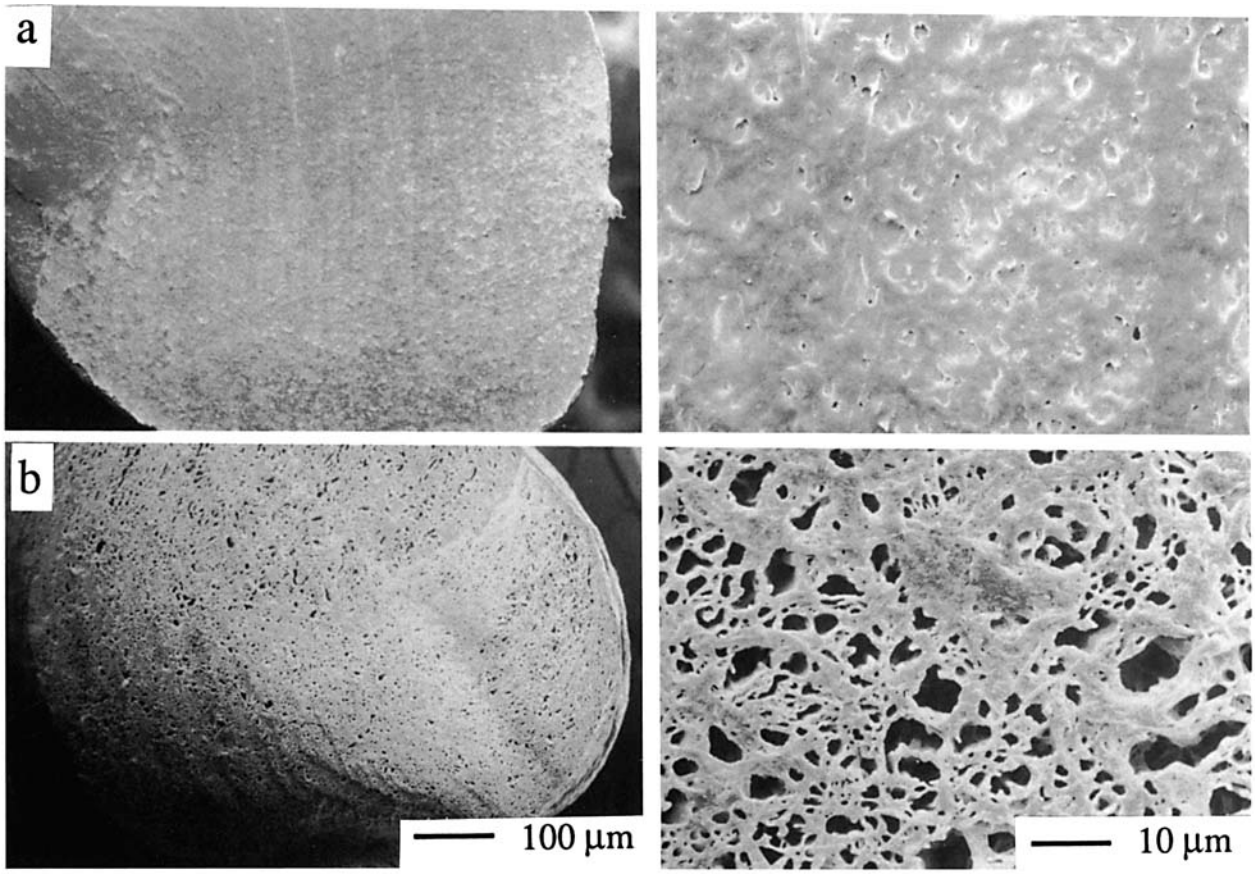

Figure 14 Scanning electron micrographs of (a) untreated and (b) α-amylase etched fracture surfaces of a WM70 filament. Images on the right represent magnified views of the images on the left. Foaming is evident in the untreated filament. Large-scale removal of the starch-rich domains occurs during enzymatic etching.

for the NC blends containing less than 50% starch, but only erosion of the filament fracture surface was observed for the NC70 and NC85 filaments. For the NC30 and NC50 blends, roughly spherical domains were visible after etching. These cavities ranged in size from 0.05 to 3 μm [Fig. 16 (a) and (b)]. The surfaces of the NC70 and some areas of the NC85 filament appear nodular, which may result from drying of a previously swollen filament [Fig. 16 (c) and (d)]. Note that these results are somewhat reminiscent of etching starch-based films and fibers with boiling water.[72,73]

Little morphological information was obtainable from etching of the HY blends. No differences between unetched and etched HY30 and HY50 filaments was observed [Fig. 17(a) and (b)]. The dark areas appearing in the micrograph were most likely due to holes in the gold–palladium coating which were observed due to loss of volatiles (i.e., water vapor, scission products) from the blend during exposure to the electron beam.[74] The HY70 and HY85 blends also did not show much etching behavior [Fig. 18(c) and (d)], but some changes in the surface structure most likely attributable to swelling and subsequent drying of the structure were evident.

Since the α-amylase etchant will attack the α(1,4)-glycosidic linkage and not the α(1,6) linkage, it was not expected that the WM blends would etch the most easily. The NC series showed some removal of the starch-rich domains at compositions less than 50% starch, but at higher compositions, little etching was observable. Surprisingly, the HY blends with almost all α(1,4) linkages showed the most resistance to etching. This can be understood in terms of the accessibility of the etchant to the starch, crystallinity of starch, and the use of water as a carrier for the enzyme etchant. The extent of etching relies on the susceptibility of the blend to the penetration of the aqueous carrier phase. The diffusion of water and access of the water-soluble enzymes into a blend is expected to be less for a miscible starch–EVOH region than for a pure starch domain. Therefore, compatibility of starch with the EVOH component may diminish some of the ability of the blend to etch and

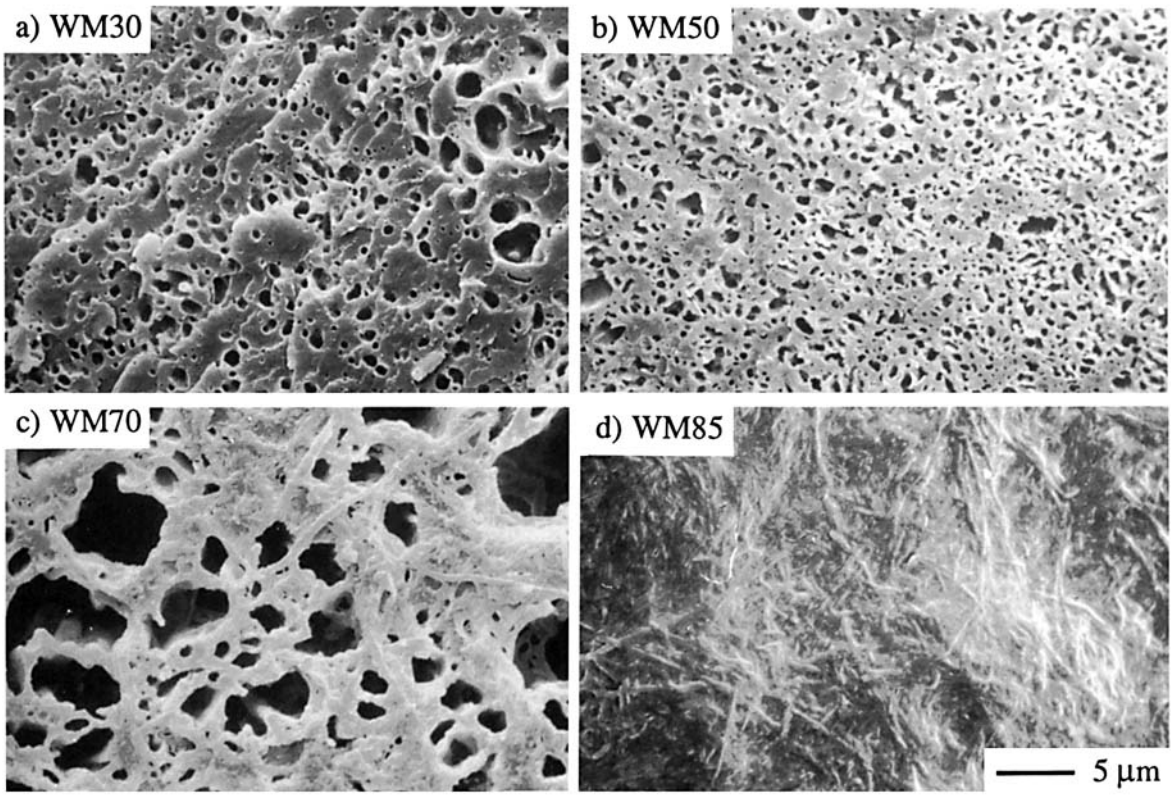

Figure 15 Scanning electron micrographs of α-amylase etched fracture surfaces of (a) WM30, (b) WM50, (c) WM70, and (d) WM85 extrudates. Discrete starch domains are evident at compositions less than 50% starch. EVOH-rich fibrils are observable at higher starch compositions. Collapse of the WM85 filament occurred during etching and EVOH-rich filaments are present in the collected residue.

domains will become less evident. Also, if certain components are crystalline, etching will be retarded in the crystalline regions compared to the amorphous regions. At lower compositions of the starch component, the fraction of domains accessible to the etchant decreases and the fraction of isolated clusters increases, thus making etching less effective. Treatment of the 100% starch blends with water showed complete collapse of the WM100 filament, swelling of the NC100, and slight swelling of the HY100 filaments. Treating the same blends with enzyme solution results in breakup of the WM100 and NC100 filaments and slight swelling of the HY100 filament. Because of the sensitivity of the waxy maize to water, etching of the starch-rich domains in the WM blends can be carried out even in the control water solution. The addition of the enzyme, however, has resulted in greater removal of polymer, possibly by scissioning any chains that have become entangled and allowing lower molecular weight chains to be carried into solution. Studies by others[75] have also demonstrated that the susceptibility of native granules is dependent upon the relative amounts of amylose and amylopectin present in the starch; high-amylose varieties are less readily attacked by enzymes (because of increased H-bonding and retrogradation[76,77]) whereas WM varieties are most susceptible.

TEM provided more detailed information on the blend morphology of the starch/EVOH blends.[34] Micrographs of the WM50, NC50, and HY50 blends are shown in Figure 18 which illustrate the existence of distinct starch-rich domains for each of the starch varieties employed in this study (iodine-stained starch-rich domains appear dark against the lighter EVOH-rich matrix via mass thickness contrast). For the WM blend (WM50), a phase-separated structure reminiscent of an incompletely mixed incompatible polymer was observed [Fig. 18(a)]. Oriented droplets ranging from 0.05 μm to approximately 5 μm in length were visible with L/D values averaging 1.8 $\pm$ 0.5 (smallest droplets are least oriented, as expected). Irregularities in droplet shape and the fact that these droplets exhibited some preferred orientation indicates that optimum blending between the two polymer components was not achieved dur-

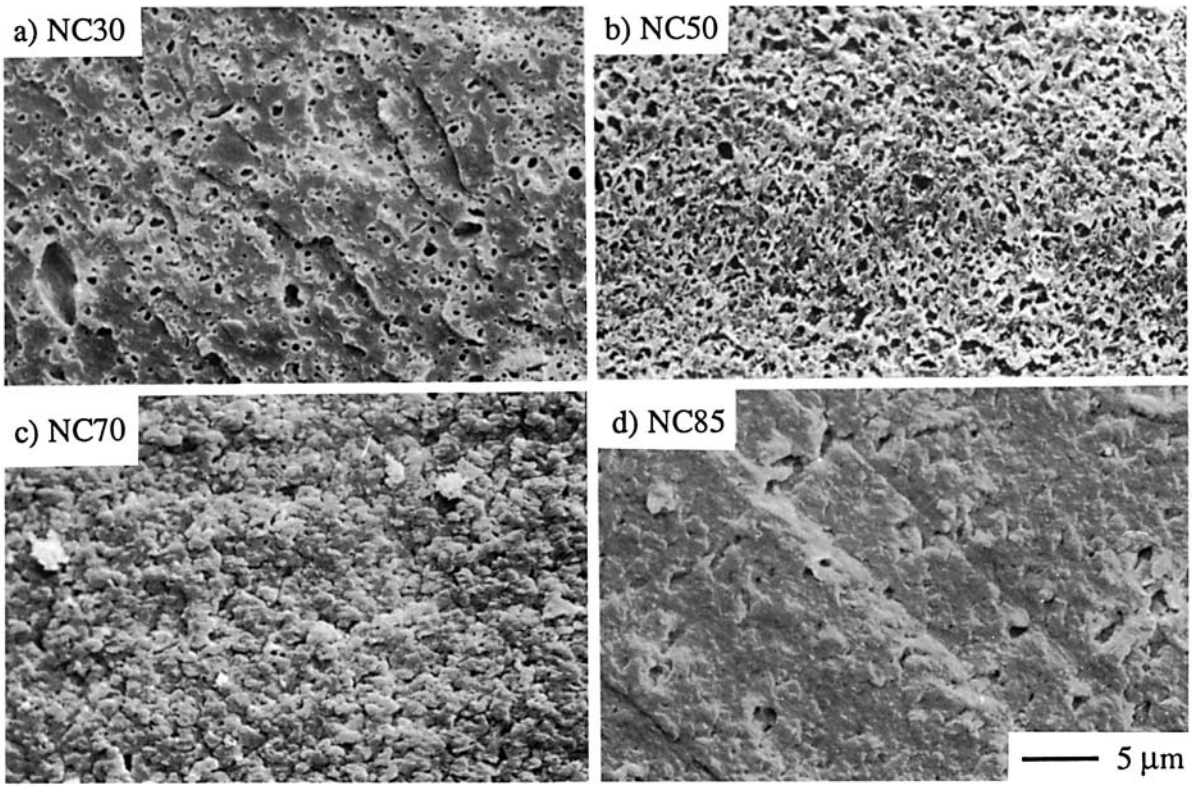

Figure 16 Scanning electron micrographs of α-amylase-etched fracture surfaces of (a) NC30, (b) NC50, (c) NC70, and (d) NC85 extrudates. Discrete starch-rich domains are present in the NC30 filament. Starch removal occurs in the NC50 blend, but domains are less discrete. Etching of filaments containing more than 50% starch is less effective at distinguishing between starch-rich and EVOH-rich domains.

ing the extrusion process.[78] Smaller light-phase domains appear within the darker regions, indicating the formation of composite droplets. Domain sizes are consistent with those observed in SEM for the etched WM50 blend [Fig. 15(b)].

Unlike in the WM50 blend, no composite droplets were observed in the NC50 blend [Fig. 18(b)]. The EVOH-rich, lighter area, appeared continuous throughout the sections, indicating that this component (or a mixture of mostly EVOH and some of the starch fraction) forms the matrix. Starch-rich domains were visible as discrete domains ranging in size from approximately 0.05 to 1.2 μm. Although the electron densities of the WM and NC starches are similar, the contrast between the starch-rich domains and the blend matrix is lower. This fact may indicated that the amylose fraction in the NC starch may be partially miscible with the EVOH fraction.

Finally, the HY50 blend exhibits a finer dispersion of smaller starch-rich domains ($d < 0.25$ μm) distributed throughout a gray matrix [Fig. 18(c)]. Overall, HY blends are more difficult to visualize due to the lower initial contrast level between the starch-rich and EVOH-rich domains which quickly fades as the sample is observed in TEM. This lower contrast as well as finer domain sizes provides evidence for even greater levels of miscibility between the starch and EVOH components. The presence of visibly discrete starch-rich domains, however, indicates that, for the most part, all the starch types in this study are somewhat immiscible with EVOH. (It should be noted that the level of starch/EVOH contrast evident in WM, NC, and HY blends is also observed to decrease in blend sections that have not been stained. Thus, the observed contrast differences are not merely due to iodine uptake variations among the starch types.)

The addition of EVOH will affect the extent to which the starch component will be sheared during the extrusion process. Rheological measurements from Villar et al.[32] can be used to further understand our structural observations. Capillary viscometry measurements showed that the viscosity of the blends generally decreases as the EVOH content increases (except for the WM blends). At 150°C and a shear rate of 100 s^{-1}, EVOH, WM100, NC100, and HY100 have viscosities of 900, 320, 1000, and 5100 Pa-s, respectively. At compositions of more than

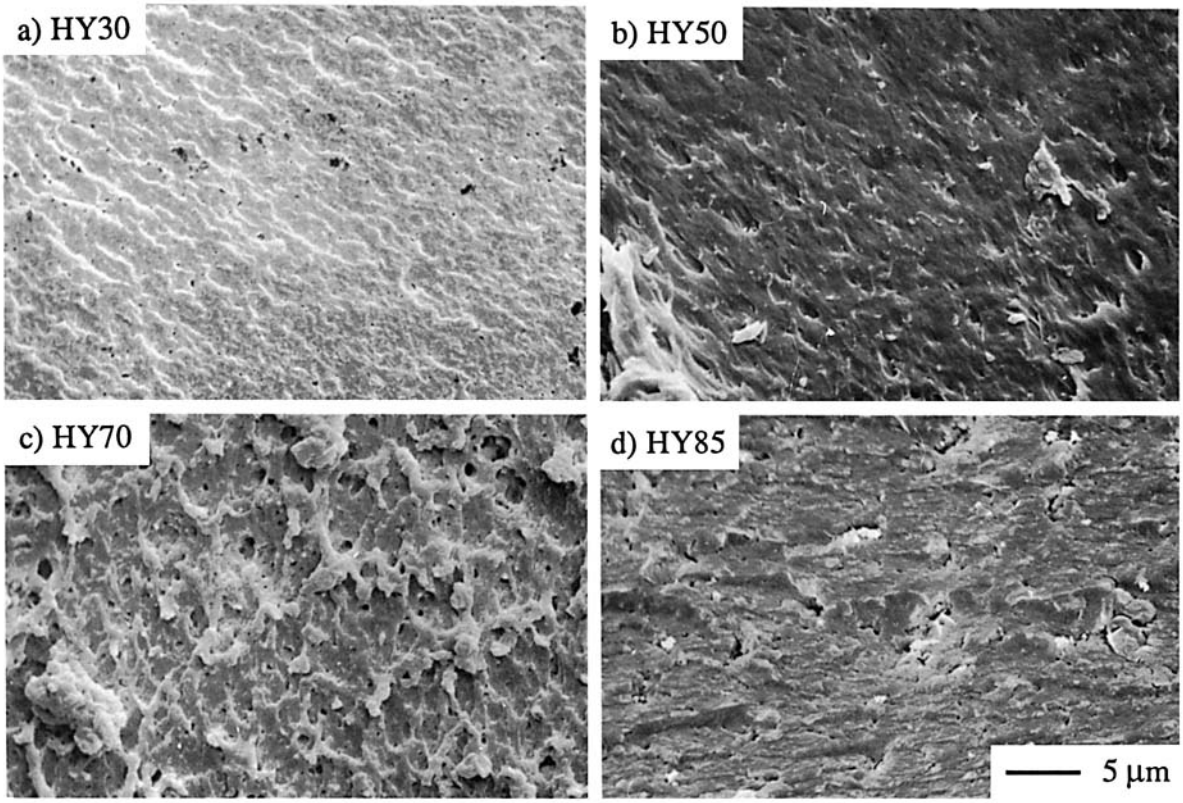

Figure 17 Scanning electron micrographs of α-amylase-etched fracture surfaces of (a) HY30, (b) HY50, (c) HY70, and (d) HY85 extrudates. The etchant had no effect on blends containing less than 50% starch. Some texture development in blends containing more than 50% starch occurred, but domains corresponding to EVOH-rich or starch-rich compositions are not distinguishable.

50% EVOH, the viscosity of the blends tends to approach that of neat EVOH. Villar et al. proposed that the starch molecules experience lower stress at these compositions and undergo less chain scission during the compounding process. This behavior will have direct consequences on the mixing behavior between the starch and EVOH components. SEM on the WM series has shown that distinct starch-rich domains are evident for the 30, 50, and 70% compositions. For WM50, the blend structure is similar to that of traditional incompatible polymer blends, whereas for blends with high starch contents, the minority EVOH component appeared to be well distributed throughout the starch matrix. For the NC blends, discrete starch domains were evident at compositions less than 50% starch; however, no discrete phases were evident in SEM. (Further TEM of the NC series, shows that, similar to the WM blends, EVOH is finely dispersed in blends high in starch content.[34]) For the HY blends, the viscosity of the starch is much higher than that of the EVOH component; however, finer mixing of the phases is evident. As demonstrated in the viscometry data, incorporation of EVOH into the blend lowers the viscosity of the material even at relatively high amylose content. This observation is consistent with the results of this morphology study in which the EVOH and HY appear to have the most interaction.

Phase Coarsening of Starch/EVOH Blends

A study was performed on the WM30 blend pellets in order to understand more about the stability of the phase structure of starch blends in the melt. This property is extremely relevant to processing applications such as injection molding, film blowing, and fiber spinning where holding time in the melt becomes very important. Pellet sections ($\sim$ 25 mg) were heated in the DSC (in high-pressure capsules, with a nitrogen purge) to 150°C at a rate of 10°C/min, held at that temperature for 0.01, 0.1, 1.0, 10, 100, and 1000 min, and cooled at the maximum DSC-7 cooling rate (set to 500°C/min). DSC results showed consistent sample-to-sample melting behavior. The samples were then removed from the DSC capsules, placed in liquid nitrogen for 1 min,

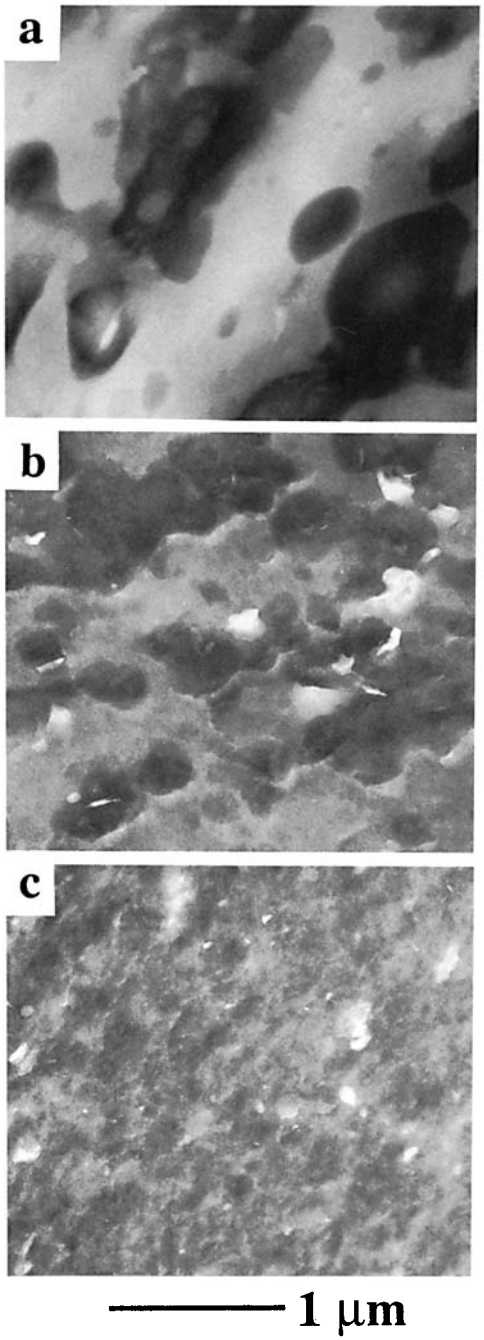

Figure 18 Transmission electron micrographs of iodine stained starch/EVOH (50 : 50) blends: (a) WM50; (b) NC50; (c) HY50 extrudate sections.

and then immediately fractured using a razor blade to initiate the crack. One section was viewed in SEM as fractured. The other section of each fracture was etched with α-amylase before viewing in the SEM. Both sections were coated with Au—Pd before imaging in the microscope.

As shown in Figure 19, domain growth of the WM-rich fraction was observed. However, images of the some of the control samples show voids inherent in the pellets which may have formed during their initial processing or in the thermal treatment. These voids (from volatile foaming) may have facilitated the etching behavior of some of the pellets, resulting in artifacts inherent in the observed systems. Because of this inherent phenomena, a quantitative analysis of the domain growth will be in error. Estimates of average void size as a function of time are 0.9, 1.2, 1.5, 1.5, 2.8, and 3.8 $\pm$ 0.2 μm over the time range; this behavior does not follow Ostwald ripening kinetics for nucleation and growth of minority-phase domains (i.e., $d \neq t^{1/3}$) as has been observed for other polymer blends.[79] Instead, a slower rate of coarsening ($d \sim t^{1/8}$) is observed, which may be a result of the initial phase sizes present upon exiting the extruder, diffusional properties of the starch-domains at 150°C (partially due to the high molecular weight of the starch component), interfacial effects involving the processing additives, partial miscibility of components, and plasticizer migration in the blend.

SEM of Etched Filaments—Effect of Capillary Flow

To gain some insight on the bulk morphological structure that forms when molten starch/EVOH blends are forced through a capillary to form a filament, the surfaces, axial cross sections, and longitudinal cross sections of certain filaments were examined. Results for the WM30 and WM70 blends are shown in Figures 20 and 21, respectively. On the left side of each figure are untreated surfaces; on the right side are the results of enzymatically etching the filament (with exposed surfaces) following the procedure given previously.

The etching procedure appeared to have little effect on the outside surfaces of starch/EVOH filaments. The WM30 filament surface was highly textured with nodular and oblong protuberances ranging in size from 1 to 10 microns which indicate inhomogeneity in the sample flow [Fig. 20(a)]. Etching with enzymatic solution does not appear to dramatically change the appearance of the filament surface, although some oblong holes (up to 5 μm long) and cracks extending along the flow direction are visible. Sharking or ribbing of the WM70 filament surface was observed [Fig. 21(a)]; this was a result of unstable flow through the spinnerette.[48] The etched WM70 filament also possessed some holes and grooves but its appearance was still strongly reminiscent of the original filament.

As evident in Figures 20(b) and 21(b), which show the axial cross sections of the filaments, some foam-

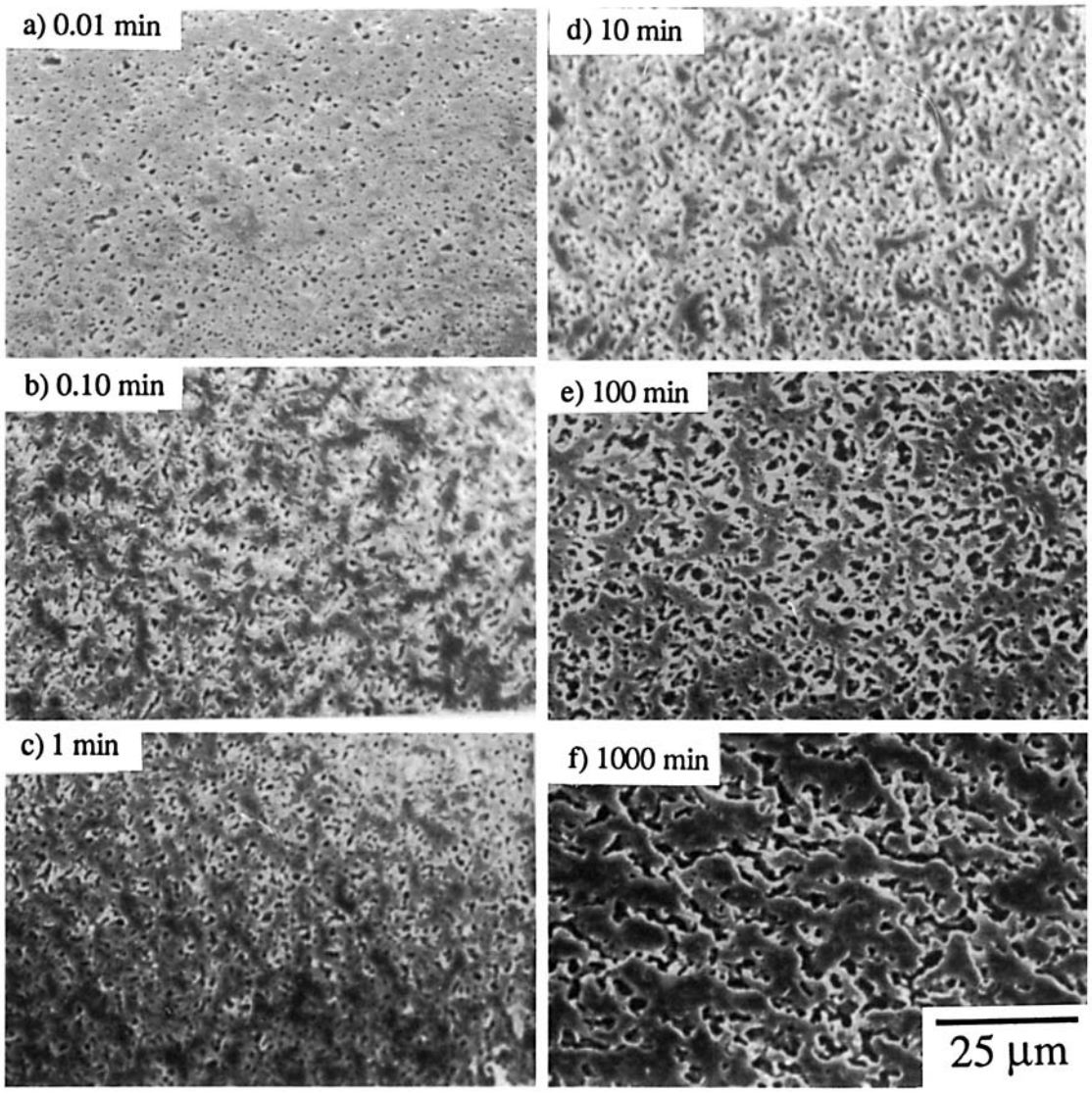

Figure 19 Scanning electron micrographs of WM30 extrudate that has been held at 150°C for (a) 0.01 min, (b) 0.1 min, (c) 1 min, (d) 10 min, (e) 100 min, and (f) 1000 min. Samples were etched with α-amylase aqueous solution prior to viewing in the microscope.

ing had occurred in the WM30 blend and more extensively in the WM70 filament. Both fracture surfaces appear very different after etching. In the axial cross-sectional view, the WM30 filament contained approximately circular domains ranging in size from 0.2 to 3 μm [Fig. 20(b)]. The WM70 filament possessed many irregularly shaped domains that ranged in size from 0.5 to 17 μm. The longitudinal cross-sectional view of the WM30 filament indicated that the starch-rich domains were ellipsoidal in shape and are aligned along the fiber axis. Values for L/D range from 1 to greater than 10. Phase inversion appears to occur in the WM70 sample. Here, the EVOH phase forms long threadlike particles. These threads are connected together horizontally, possibly indicating a co-continuous structure since the minority EVOH component appears to extend throughout the length of the sample. It should be noted that there is no evidence from flat film WAXS that the EVOH or starch phases are oriented; this result indicates that, though the phases are oriented, the molecules contained in the domains have relaxed.

Structural Influences on Starch/EVOH Blend Processability and Properties

During the compounding of the model series of blends, adequate amounts of plasticizer (glycerin and water) as well as sufficient levels of heat and shear

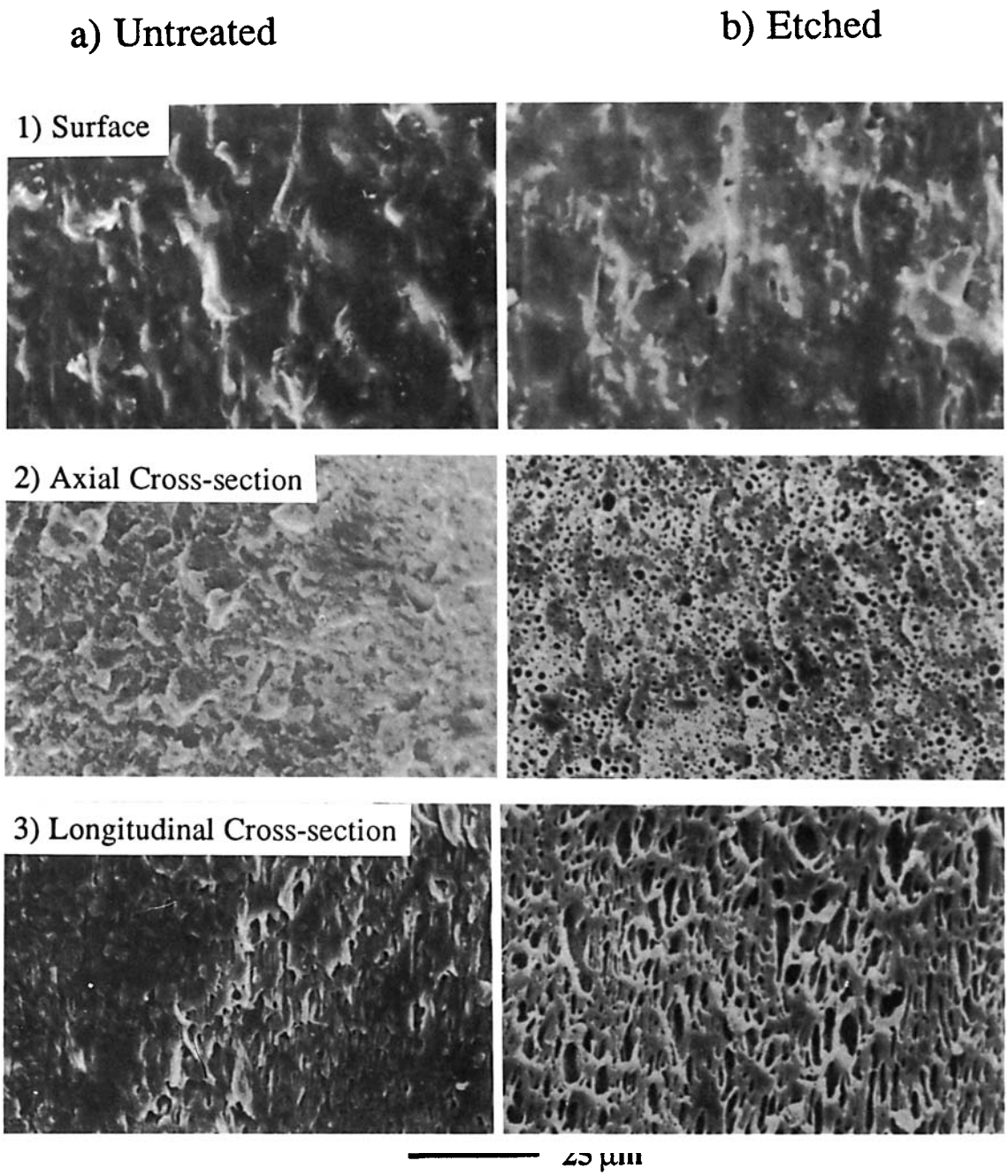

Figure 20 Scanning electron micrographs of various surfaces of a WM30 filament (d = 710 μm): (1) surface; (2) axial cross section; (3) longitudinal cross section. Draw direction is vertical (draw ratio = 1). Images on the left (a) are of untreated filaments. Images on the right (b) are similar filaments which have been etched with α-amylase aqueous solutions.

allowed for the destructurization of the initial granules. SEM and TEM showed no trace of intact native granules for all of the WM and NC starch blends. X-ray and thermal analysis confirmed that the starch component formed a molten phase during the compounding process as evident in the loss of crystallinity in the amylopectin component. Partial miscibility of the amylose fraction is also suggested due to etching behavior and melting-point depression of the EVOH component. The distribution and connectivity of starch-rich phase domains which are smaller than granule size will alter the transport processes leading to biodegradation of the blend.

Crystallinity in the NC and HY blends occurs in both the EVOH and starch domains. An increase in crystallinity will lower the rate of biodegradation

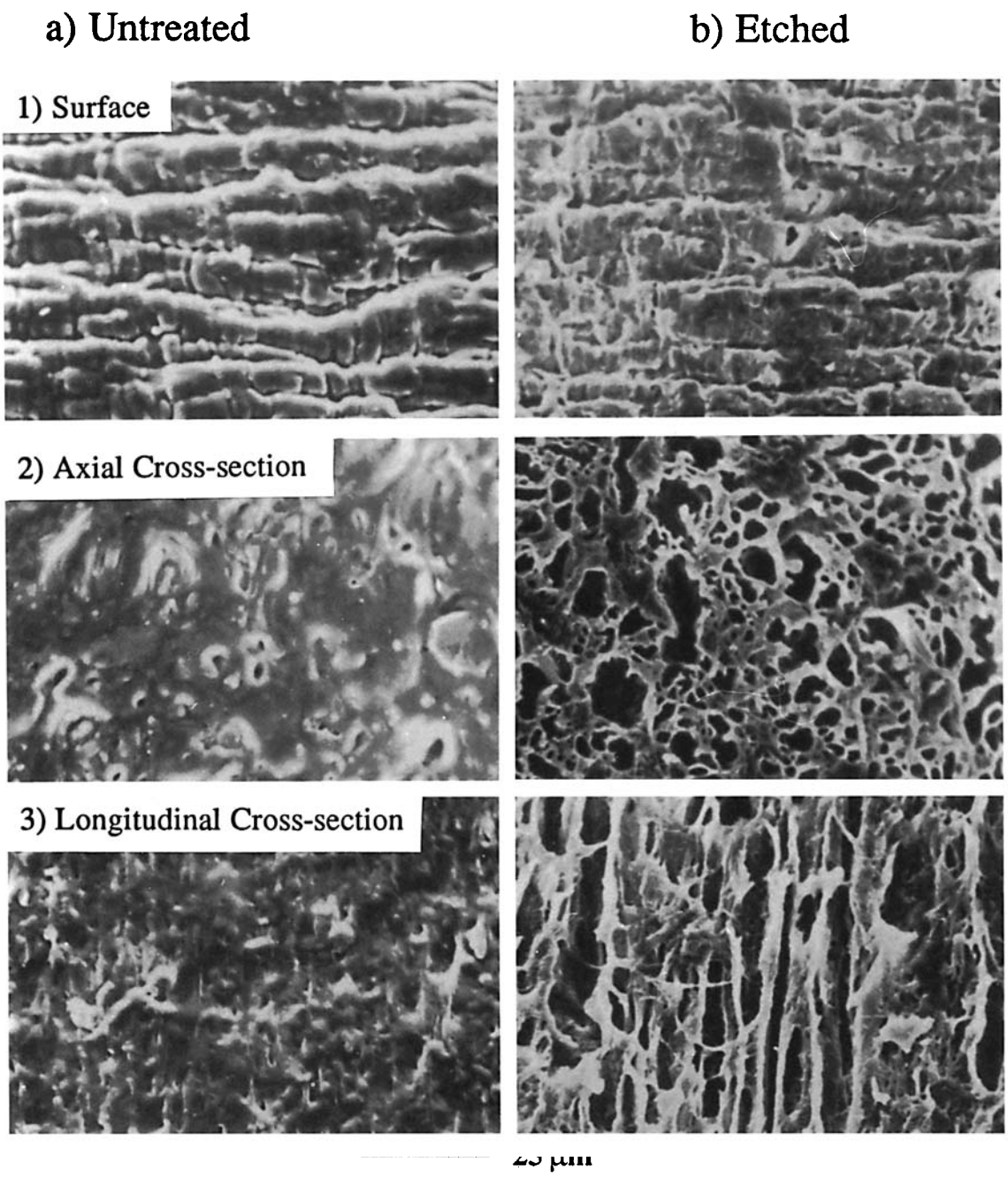

Figure 21 Scanning electron micrographs of various surfaces of a WM70 filament (d = 1080 μm): (1) surface; (2) axial cross section; (3) longitudinal cross section. Draw direction is vertical (draw ratio = 1). Images on the left (a) are of untreated filaments. Images on the right (b) are similar filaments which have been etched with α-amylase aqueous solutions.

for these types of blends. As noted from the etching studies, the aqueous solutions do not penetrate the HY extrudates or filaments and the α-amylase does not readily etch the starch phase from the bulk structure. Similar results should occur with microbial attack. In solution, amylose, more than amylopectin, undergoes a phenomenon called retrogradation in which interchain hydrogen bonding between polymer chains causes them to precipitate out of aqueous solutions.[80] This action of the amylose chains would serve to exclude plasticizer from "retrograded" regions. Plasticizer was observed on the outer surface of the HY blends which seems to confirm this hypothesis. Retrogradation of amylopectin is also documented to occur but much more slowly over time.[76,80] This process contributes to the small

endotherm observed in DSC between 55 and 60°C for the NC and WM blends (note that most of this endotherm is, however, attributed to the additive) and will increase the brittleness and slow the rate of biodegradation for these blends.

Under certain processing conditions (i.e., filament formation), EVOH has been shown to primarily coat the blend surfaces as is evident in the enzymatic etching experiment (similar results are evident in studies employing cross-sectional TEM of starch/EVOH fibers[34]). EVOH is more moisture-resistant and less biodegradable than is starch. Articles made with this coating will therefore be less moisture-sensitive and initially more resistant to microbial attack.

The mechanical properties of starch/EVOH blends will also depend the distribution of starch-rich and EVOH-rich phases. Smaller and well-distributed phase domains will lead to mechanical behavior that is more consistent with a blend of two components (i.e., load is more uniformly distributed). Conversely, large domains of starch will more likely act as points of concentration for stress, resulting in mechanical failure at lower tensile stresses. Thus, blends can contain higher amounts of destructurized starch rather than dry starch granule filler. If miscibility exists between starch and EVOH, the interfacial adhesion between phases may improve, and debonding of domains from the matrix, leading to failure, is expected to decrease. Finally, blends containing more amylose are more likely to be stronger, partially due to the larger amount of linear, crystallizable polymer present. The mechanical behavior of the starch/EVOH blends is explored in more detail in a separate study.[33]

CONCLUSIONS

The extrusion blending of three varieties of corn starch with poly(ethylene–vinyl alcohol) (EVOH) to produce a biodegradable thermoplastic resin was investigated by examining the structural characteristics of the resulting blends. The corn starches, Waxy Maize (WM), Native Corn (NC), and high-amylose Hylon VII (HY), varied in their branch content (amylose-to-amylopectin ratio) and molecular weight. The starches were blended with EVOH containing 56 mol % VOH over a systematic compositional range from 100% starch to 0% starch (control sample). Glycerin and water were employed as plasticizers.

X-ray, thermal analysis, and electron microscopy results indicated that the WM and NC granules were destructurized during the extrusion process (the HY starch was pretreated prior to blending), and a polymer–polymer blend was formed with the EVOH component. All the blends showed evidence of phase separation between starch and EVOH. The NC and HY blends, in particular, appeared to be partially miscible as evident from EVOH melting-point depression beyond the effects due to the two plasticizers alone, smaller domain sizes, and lower contrast between phases in TEM. Blends containing amylose exhibited crystalline scattering patterns associated with the amylose complex in WAXS, although most of the crystallinity was due to the EVOH component.

Whereas WM blends are most susceptible to moisture and enzyme-etching treatments, the NC and HY blends showed more resistance to swelling, dissolution, and degradation due to increased levels of crystallinity, H-bonding in the starch fraction, smaller phase sizes, and partial miscibility with the EVOH component. SEM was the most useful for studying WM blends and NC blends with starch contents of 50% or less. More morphological information was attainable with TEM (using iodine as a stain for starch) in which distinct starch-rich and EVOH-rich domains were clearly evident for all three starch types. Starch-rich domain sizes decreased as the amylose content of the starch component was increased (i.e., $d_{WM50} > d_{NC50} > d_{HY50}$) and contrast between phases decreased, indicating increased miscibility between the polymer components. At least four polymer phases are formed in these systems: (1) amorphous starch, (2) amorphous EVOH; (3) crystalline amylose, and (4) crystalline EVOH. Phase separation of the amylose and amylopectin components in amorphous starch is also likely due to branching and molecular weight differences.

The influence of time in the melt and shear (capillary) flow on the phase morphology for select WM blends was then examined since this series yielded the most structural information with SEM. WM-rich domains undergo phase coarsening as a function of time in the melt, although much slower than Ostwald ripening kinetics ($d \sim t^{1/8}$). Orientation of both starch-rich and EVOH-rich domains, but not molecules, was observed at various compositions; EVOH underwent significant orientation relative to starch as evident by EVOH-rich fibrils in blends with a large amount of starch. Little etching was observed on the filament surfaces, indicating that EVOH is coating the specimen as it is extruded through a capillary.

The authors thank Novon Products, Warner-Lambert Corp., for supplying materials, compounding the blends,

and providing initial seed funding for this project. Acknowledgment is made to the Center for Materials Science and Engineering at MIT for use of its electron microscope and X-ray diffraction facilities. The Department of Civil Engineering is also acknowledged for allowing us to use their scanning electron microscope. Funding was provided by the U.S. Department of Agriculture (Grant # 91-COOP-2-6108). S. S. also acknowledges the National Science Foundation for providing a graduate fellowship.

REFERENCES

1. R. L. Whistler, in *Starch: Chemistry and Technology,* R. L. Whistler, J. N. Bemiller, and E. F. Paschall, Eds., Academic Press, New York, 1984, p. 1.
2. W. M. Doane, in *New Crops, New Uses, New Markets: Industrial and Commercial Products from U.S. Agriculture,* U.S. Dept. of Agriculture, Washington, D.C., 1992, p. 147.
3. J. W. Mullen and E. Pacsu, *Ind. Eng. Chem.,* **35,** 381 (1943).
4. I. Tomka, PCT Pat. WO 90/05161 (1989).
5. F. H. Otey, R. P. Westhoff, and C. R. Russell, presentation at Technical Symposium: Nonwoven Product Technology, 1975.
6. F. H. Otey, R. P. Westhoff, and C. R. Russell, *Ind. Eng. Chem. Prod. Res. Dev.,* **16,** 305 (1977).
7. R. P. Westhoff, W. F. Kwoleck, and F. H. Otey, *Starch/Starke,* **31,** 163 (1979).
8. G. F. Fanta, R. C. Burr, and W. M. Doane, *J. Appl. Polym. Sci.,* **25,** 2285 (1980).
9. F. H. Otey and R. P. Westhoff, in *Proceedings of the 15th National Agricultural Plastics Congress,* 1980.
10. F. H. Otey, in *Proceedings of the 17th Nat'l Agric. Plastics Congress, "Plasticulture Worldwide,"* 1983.
11. W. M. Doane, in *First Annual Corn Utilization Conference,* 1987.
12. W. M. Doane, *Polym. Prepr.,* **28,** 103 (1987).
13. G. F. Fanta, in *Corn Utilization Conference II, National Corn Growers Association,* 1988.
14. C. L. Swanson, R. P. Westhoff, and W. M. Doane, in *Corn Utilization Conference II,* 1988.
15. C. Bastioli, V. Bellotti, L. Del Gludice, and R. Lombi, Eur. Pat. Appl. 90,110,070.1 (1990).
16. R. L. Shogren, R. V. Greene, and Y. V. Wu, *J. Appl. Polym. Sci.,* **42,** 1701 (1991).
17. R. L. Shogren, A. R. Thompson, R. V. Greene, S. H. Gordon, and G. Cote, *J. Appl. Polym. Sci.,* **42,** 2279 (1991).
18. R. L. Shogren, A. R. Thompson, F. C. Felker, R. E. Harry-O'Kuru, S. H. Gordon, R. V. Greene, and J. M. Gould, *J. Appl. Polym. Sci.,* **44,** 1971 (1992).
19. C. Ching, D. L. Kaplan, and E. L. Thomas, *Biodegradable Polymers and Packaging,* Technomics, Lancaster, PA, 1993.
20. D. Trimmell, C. L. Swanson, and R. L. Shogren, *J. Appl. Polym. Sci.,* **48,** 1665 (1993).
21. H. Roper and H. Koch, *Starch/Starke,* **42,** 123 (1990).
22. W. M. Doane, *Starch/Starke,* **44,** 293 (1992).
23. R. L. Shogren, G. F. Fanta, and W. M. Doane, *Starch/Starke,* **45,** 276 (1993).
24. J.-C. Huang, A. S. Shetty, and M.-S. Wang, *Adv. Polym. Technol.,* **10,** 23 (1990).
25. G. Swift, *Acc. Chem. Res.,* **26,** 105 (1993).
26. J. Mayer and D. L. Kaplan, *Trends Polym. Sci.,* **2,** 227 (1994).
27. F. Wittwer and I. Tomka, U.S. Pat. 4,673,438 (1987) (to Warner-Lambert Co.).
28. G. Lay, J. Rehm, R. F. Stepto, M. Thoma, J.-P. Sachetto, D. J. Lentz, and J. Silbiger, U.S. Pat. 5,095,054 (1992) (to Warner-Lambert Co.).
29. C. Bastioli, R. Lombi, G. Del Tredici, and I. Guanella, Eur. Pat. Appl. (1990).
30. E. R. George, T. M. Sullivan, and E. H. Park, *Polym. Eng. Sci.,* **34,** 17 (1994).
31. J. E. McCassie, J. M. Mayer, R. E. Stote, A. E. Shupe, P. J. Stenhouse, P. A. Dell, and D. L. Kaplan, in *Biodegradable Polymers and Packaging,* C. Ching, D. L. Kaplan, and E. L. Thomas, Eds., Technomic, Lancaster, PA, 1993, p. 217.
32. M. A. Villar, E. L. Thomas, and R. C. Armstrong, to appear.
33. S. Simmons, PhD Dissertation, Massachusetts Institute of Technology, Cambridge, MA (1995).
34. S. Simmons and E. L. Thomas, to appear.
35. D. R. Paul and S. Newman, *Polymer Blends,* Academic Press, New York, 1978.
36. R. Billmers, Personal communication, National Starch Co., Bridgewater, NJ, 1994.
37. R. Dolfinger, Unpublished data, 1993.
38. *Constant Test Atmospheres over Aqueous Solutions,* Deutsche Normen, 1981.
39. W. Ruland, *Acta Crystallogr.,* **14,** 1180 (1961).
40. L. E. Alexander, *X-ray Diffraction Methods in Polymer Science,* Wiley, New York, 1969.
41. C. H. MacFillavry and G. Riech, *International Tables for X-ray Crystallography,* Kynoch Press, Birmingham, England, 1968.
42. D. L. Misell, *Image Analysis, Enhancement and Interpretation,* North-Holland, New York, 1978.
43. L. L. Buckholz, Jr., *Cereal Foods World,* **33,** 547 (1988).
44. W. Wiedmann and E. Strobel, *Compounding of Thermoplastic Starch with Twin-Screw Extruders,* Werner-Pfleiderer Corp., 1992.
45. W. Wiedmann, *Principles and Applications of Starch Extrusion,* Werner-Pfleiderer Corp., 1992.
46. L. Elsberg, unpublished results, 1993.
47. C. E. Weigand, MS Thesis, Massachusetts Institute of Technology, 1992.
48. Z. Tadmor and C. G. Gogos, *Principles of Polymer Processing,* Wiley, New York, 1979.
49. A. Sarko and H.-C. H. Wu, *Starch/Starke,* **30,** 73 (1978).
50. H. F. Zobel, *Starch/Starke,* **40,** 1 (1988).
51. P. Muhrbeck, *Starch/Starke,* **43,** 347 (1991).
52. C. Mercier, R. Charbonniere, D. Gallant, and A. Guilbot, in *Polysaccharides in Food,* J. M. V. Blanshard

and J. R. Mitchell, Eds., Butterworth, London, 1979, p. 153.
53. P. Colonna, J. L. Doublier, J. P. Melcion, F. de Monredon, and C. Mercier, *Cereal Chem.*, **1,** 538 (1984).
54. J. R. Katz, in *Zeitshrift fur Physikalische Chemie,* W. Ostwald and J. H. Van't Hoff, Eds., Akademische Veraggellschaft, Leipzig, 1930.
55. H.-C. H. Wu and A. Sarko, *Carbohydr. Res.*, **54,** C3 (1977).
56. H.-C. H. Wu and A. Sarko, *Carbohydr. Res.*, **61,** 27 (1978).
57. T. J. Schoch, *J. Am. Chem. Soc.*, **64,** 2954 (1942).
58. P. L. Russell, *Starch/Starke,* **35,** 277 (1983).
59. P. Colonna, J. Tayeb, and C. Mercier, in *Extrusion Cooking,* C. Mercier, P. Linko, and J. M. Harper, Eds., American Association of Cereal Chemists, St. Paul, MN, 1989, p. 247.
60. C. Mercier, R. Charbonniere, J. Grebaut, and J. F. de la Gueriviere, *Cereal Chem.*, **57,** 4 (1980).
61. M. Ahmed and J. Lelievre, *Starch/Starke,* **30,** 78 (1978).
62. J. R. Katz, *Baker's Week.*, **81,** 34 (1934).
63. R. D. Dragsdorf and E. Varriano-Marston, *Cereal Chem.*, **57,** 310 (1980).
64. K. J. Zeleznak and R. C. Hoseney, *Starch/Starke,* **39,** 231 (1987).
65. J. Longton and G. A. LeGrys, *Starch/Starke,* **33,** 410 (1981).
66. R. L. Shogren, *Carbohydr. Polym.*, **19,** 83 (1992).
67. R. L. Evangelista, Z. L. Nikolov, W. Sung, J.-L. Jane, and R. J. Gelina, *Ind. Eng. Chem. Res.*, **30,** 1841 (1991).
68. R. P. Westhoff, F. H. Otey, C. L. Mehltretter, and C. R. Russell, *Ind. Eng. Chem. Prod. Res. Dev.*, **13,** 123 (1974).
69. G. J. L. Griffen, *Adv. Chem. Ser.*, **134,** 156 (1974).
70. L. Engel, H. Kingele, G. W. Ehrenstein, and H. Schaper, *An Atlas of Polymer Damage: Surface Examination by Scanning Electron Microscope,* Prentice-Hall, Englewood Cliffs, NJ, 1981.
71. P. Bernfield, *Methods Enzymol.*, **1,** 149 (1955).
72. C. Bastioli, presentation at Environmentally Degradable Polymers: Technical, Business, and Public Perspectives August 13–15, 1991.
73. S. Simmons, C. E. Weigand, R. J. Albalak, R. C. Armstrong, and E. L. Thomas, in *Biodegradable Polymers and Packaging,* D. L. Kaplan, C. Ching and E. L. Thomas, Eds., Technomic, Lancaster, PA, 1993, p. 171.
74. L. Reimer, *Lab. Invest.*, **14,** 344 (1965).
75. A. D. Evers, in *Food Microscopy,* J. G. Vaughan, Ed., Academic Press, New York, 1979, p. 139.
76. M. J. Miles, V. J. Morris, P. D. Orford, and S. G. Ring, *Carbohydr. Res.*, **135,** 271 (1985).
77. M. Gudmundsson and A. C. Eliasson, *Carbohydr. Polym.*, **13,** 295 (1990).
78. D. R. Paul and S. Newmann, *Polymer Blends,* Academic Press, New York, 1978.
79. F. M. Mirabella, Jr., *J. Polym. Sci. Part B Poly. Phys. Ed.*, **32,** 1205 (1994).
80. H. J. Cornell, *Starke,* **43** (1963).

Received April 19, 1995
Accepted June 9, 1995